

Review

Recent Advances in Lateral Flow Assays for Viral Protein Detection with Nanomaterial-Based Optical Sensors

Min Jung Kim ¹, Izzati Haizan ², Min Ju Ahn ³, Dong-Hyeok Park ¹ and Jin-Ha Choi ^{1,2,*} 

¹ School of Chemical Engineering, Clean Energy Research Center, Jeonbuk National University, 567 Baekje-daero, Deokjin-gu, Jeonju-si 54896, Jeollabuk-do, Republic of Korea; minjeong413@jbnu.ac.kr (M.J.K.); 201610776@jbnu.ac.kr (D.-H.P.)

² Department of Bioprocess Engineering, Jeonbuk National University, 567 Baekje-daero, Deokjin-gu, Jeonju-si 54896, Jeollabuk-do, Republic of Korea; izzatihaizan22@jbnu.ac.kr

³ Department of Biotechnology, Jeonbuk National University, 79 Gobongro, Iksan-si 54596, Jeollabuk-do, Republic of Korea; ahnminju@jbnu.ac.kr

* Correspondence: jhchoi@jbnu.ac.kr

Abstract: Controlling the progression of contagious diseases is crucial for public health management, emphasizing the importance of early viral infection diagnosis. In response, lateral flow assays (LFAs) have been successfully utilized in point-of-care (POC) testing, emerging as a viable alternative to more traditional diagnostic methods. Recent advancements in virus detection have primarily leveraged methods such as reverse transcription–polymerase chain reaction (RT-PCR), reverse transcription–loop-mediated isothermal amplification (RT-LAMP), and the enzyme-linked immunosorbent assay (ELISA). Despite their proven effectiveness, these conventional techniques are often expensive, require specialized expertise, and consume a significant amount of time. In contrast, LFAs utilize nanomaterial-based optical sensing technologies, including colorimetric, fluorescence, and surface-enhanced Raman scattering (SERS), offering quick, straightforward analyses with minimal training and infrastructure requirements for detecting viral proteins in biological samples. This review describes the composition and mechanism of and recent advancements in LFAs for viral protein detection, categorizing them into colorimetric, fluorescent, and SERS-based techniques. Despite significant progress, developing a simple, stable, highly sensitive, and selective LFA system remains a formidable challenge. Nevertheless, an advanced LFA system promises not only to enhance clinical diagnostics but also to extend its utility to environmental monitoring and beyond, demonstrating its potential to revolutionize both healthcare and environmental safety.

Keywords: lateral flow assay (LFA); optical sensing; nanomaterial; virus detection; viral protein



Citation: Kim, M.J.; Haizan, I.; Ahn, M.J.; Park, D.-H.; Choi, J.-H. Recent Advances in Lateral Flow Assays for Viral Protein Detection with Nanomaterial-Based Optical Sensors. *Biosensors* **2024**, *14*, 197. <https://doi.org/10.3390/bios14040197>

Received: 15 March 2024

Revised: 12 April 2024

Accepted: 15 April 2024

Published: 17 April 2024



Copyright: © 2024 by the authors. Licensee MDPI, Basel, Switzerland. This article is an open access article distributed under the terms and conditions of the Creative Commons Attribution (CC BY) license (<https://creativecommons.org/licenses/by/4.0/>).

1. Introduction

Viruses consist of a structure with a genome inside a protein-based shell that reproduces inside hosts. Scientists have estimated that there are approximately 10^{31} viruses living on Earth [1,2]. The replication of the viral genome occurs only inside living cells (hosts), and the hosts can be any of the major cell organisms (prokaryotes, eukaryotes) [2]. Viral infectious diseases are caused by several factors, including evolutionary and adaptive genetic mutations of viruses, population growth and urbanization, population movement, global warming, and climate change, which can affect human life in many ways [3–6]. For instance, viral infectious diseases include influenza [7,8], severe acute respiratory syndrome (SARS) [9], middle east respiratory syndrome (MERS) [10,11], coronavirus disease (COVID-19) [7,12–14], acquired immune deficiency syndrome (AIDS) [15], Ebola virus disease [16], norovirus gastroenteritis [17], and Zika virus infection [18]. For example, the 1918 influenza pandemic was an extremely lethal influenza pandemic caused by the H1N1 virus. It was one of the most widespread and deadly flus witnessed by world economies, and hampered not only lives, but also society and trade-related activities. Due to this

incident, approximately 500 million people were infected by influenza, wherein one third of the world's population suffered at the time [19]. In addition, in the past few years, more than 115 million cases of infection have been confirmed worldwide since the emergence of SARS-CoV-2, and more than 2.5 million deaths have been recorded [8]. As such, since the transmission of the virus has a fatal effect on human life, an effective diagnostic method is needed to control the transmission of the virus.

In general, nucleic acid detection is performed using polymerase chain reaction (PCR) and loop-mediated isothermal amplification (LAMP). For many years, these conventional diagnostic methods have been utilized especially for virus detection. In detail, RNA virus detection techniques include reverse transcription–polymerase chain reaction (RT-PCR), reverse transcription–loop-mediated isothermal amplification (RT-LAMP), and the enzyme-linked immunosorbent assay (ELISA) [20–24]. For instance, diagnosis by real-time RT-PCR using upper respiratory tract samples is the gold standard for virus detection due to its high sensitivity and specificity [22,25–28]. On the other hand, RT-LAMP can be performed in real time by measuring turbidity or fluorescence using dyes. Real-time RT-LAMP diagnostic tests are simple and sensitive because they only require heating and visual inspection [20,29–31]. Meanwhile, in addition to nucleic acid detection, viral protein detection for virus disease detection is gaining attention due to its simplicity. This is because a single gene can express multiple proteins with various biological functions, and proteins expressed by genes can undergo various post-translational modifications. On the other hand, proteins are the final form of gene products and are directly related to biological functions. Therefore, protein biomarkers are effective for early diagnosis [32]. ELISA is a microwell plate-based assay technique that detects and quantifies proteins (antibodies, hormones, etc.). The test can be performed both qualitatively and quantitatively, and generally requires 1 to 5 h of detection [20,33–37]. In the case of sandwich ELISA, the sensitivity is very high [33]. These conventional techniques have contributed significantly to the diagnosis of several viral diseases. However, the disadvantages of being expensive, requiring skilled professionals, and requiring considerable time for the detection process have necessitated the development of affordable, accessible, and rapid viral diagnostic methods.

In line with these needs, the lateral flow assay (LFA), a paper-based technology, has emerged as an alternative for filling voids. LFAs have been successfully utilized in point-of-care (POC) diagnostic applications. It has been reported that the quantitative estimation of LFA results can significantly improve the efficiency of human and veterinary use, biological safety, consumer protection, and ecological monitoring [38]. With the advantages of being affordable, having a simple system with minimal training or infrastructure, having low temperature sensitivity, and having a short diagnostic time [20], this diagnostic platform has excellent advantages in developing and remote countries. This is due to its efficiency, especially under conditions of limited resources and scarce specially trained personnel [39,40]. Another great advantage of LFA-based testing is that it can be performed on various biological samples, including plasma, sweat, saliva, serum, urine, and whole blood. Moreover, the number of samples required for detection is much less than what is required for other conventional analyses [41]. Protein biomarkers such as virus antibodies, antigens, proteases, and surface-presenting proteins can also be detected without sample pretreatment in biological samples, such as respiratory samples taken directly from the nasopharynx, oropharynx, or saliva [42–45]. Optical sensing methods, such as colorimetric, fluorescence, and surface-enhanced Raman scattering (SERS), have a simple analysis process, high sensitivity, and selectivity, and can deliver analysis information in a convenient and inexpensive way [46]. In recent years, optical sensors using nanomaterials have been actively developed to quickly, sensitively, and specifically identify targets. Nanomaterials also have many useful properties relative to volume, such as a large surface area, a small size, a quantum confinement effect, high surface reactivity, and improved magnetic/electrical/optical properties, which can be appropriately adjusted and applied to optical sensors [47–50]. In this review, we summarize the components, structures, and principles of LFAs and present

recent advances in LFAs for detecting viral proteins by dividing methods used from 2019 to 2024 into colorimetric, fluorescence, and SERS methods.

2. LFA Components, Structures, and Principles

Generally, most LFA platforms operate on a basic working principle. The components of the LFA strip include a sample pad, a conjugate pad, a nitrocellulose (NC) membrane, and an absorbent pad that are layered together on top of a backing card (Figure 1a). LFA systems work mainly by adapting the capillary action flow rate concept in which samples containing targets flow from the sample pad along the strip to the absorbent pad. Furthermore, the role of each component in the LFA structures, its principle, and the practiced LFA formats for viral protein detection will be discussed.

The first component of LFA platforms is the sample pad. The sample pad can release analytes with high efficiency to ensure that the sample is compatible for use in subsequent inspection steps. Samples need to be processed beforehand by filtering particulates and changing their pH. This is due to the active binding of sample components and the destruction of substrate components such as mucins, which may interfere with the analysis. Some examples of sample pad materials include cellulose, glass fibers, rayon, and other filtration media. Next, the role of conjugate pads is to accommodate the target complex, keep it stable within its shelf life, and release it efficiently and reproducibly when the analysis is carried out. In detail, to ensure the optimal release and stability of the materials, the conjugate pad is pretreated beforehand through immersion in an aqueous solution of proteins, surfactants, and polymers, followed by a drying process. The materials for the conjugate pad can be glass fibers, polyester, or rayon.

Additionally, NC membranes play a crucial role in LFA platforms. The NC membrane houses two important analysis lines: a test line (T-line) and a control line (C-line). Moreover, NC membranes ensure that the target complexes flow consistently through the two lines, allowing reactions to occur and ensuring that the excess fluid, labels, and reactants escape without binding. Finally, absorbent pads are important for attracting and holding all fluids in this designated area throughout the duration of the analysis. Absorbent pads are as important as other components because, in the presence of fluid flowing opposite to the flow direction, the probability of achieving false positive results is high. Thus, for absorbent pads, high-density cellulose is generally used [51,52].

Moving forward, an in-depth working principle of the LFA platform will be explained. On the LFA strip, when a liquid sample is dropped on the sample pad, the sample will first move through the strip to the conjugate pad. Basically, on the conjugate pad, specifically tagged capture antigens or antibodies and nanoprobe such as gold nanoparticles (Au NPs), fluorophores, and quantum dots (QDs) are present. Hence, in the presence of a target in the samples, nanoprobe-detecting antigen/antibody complexes will form. After the interaction between the targets and nanoprobe, the resulting complex flows to the NC membrane, in which specific antibodies are pre-immobilized on both the T- and C-lines. On the T-line, in the presence of a target, preformed complexes on the conjugate pad will be captured by the primary immobilized antibody. Subsequently, unbound complexes from the T-line flow to the C-line and are captured by the secondary immobilized antibody, indicating that the sample solution has moved sufficiently. Finally, the absorbent pad absorbs the processed and excess samples, preventing them from flowing back to the NC membrane and conjugate pad [39,40,53–55].

In the last part of this section, the universally practiced LFA formats for viral protein detection will be introduced. Accordingly, in LFA systems, sandwich and competitive formats are typically employed (Figure 1b). Generally, the sandwich format is used to test large analytes with multiple antigenic sites, and the competitive form is applied for small-scale analyte detection, especially for analytes with low molecular weights and single antigenic determinants. In addition, the main difference between the two formats is the number of antibodies used in each LFA system. Three different types of antibodies for sandwich and two types of antibodies for competitive formats of LFA platforms are

used. First and foremost, in the sandwich formation, the three antibodies used are the nanoprobe-labeled antibody (conjugated pad), primary antibody (T-line), and secondary antibody (C-line). In the presence of a target, the nanoprobe-labeled antibody and target will form a complex on the conjugate pad. Then, the formed complex will be recognized and captured by the pre-immobilized primary antibody on the T-line, resulting in sandwich formation. Moving forward, the unbounded nanoprobe-labeled antibody will interact with the secondary antibody, resulting in an observable C-line indicating a positive result. Subsequently, the number of analytes present in the sample can be determined by the color intensity observed on the T-line. In the event of a negative result, only an observable C-line will be observed, indicating that the nanoprobe-labeled antibody interacts with the secondary antibody on the C-line. In the case of the competitive formation of the LFA system, the two antibodies used are primary (T-line) and secondary antibodies (C-line). In the event of the target's presence in the sample, the labeled analyte will compete with the target to bind with the primary antibody. Consequently, the target will bind to the primary antibody on the T-line, forming a visible red signal on the T-line. In contrast, the labeled analyte will bind to the secondary antibody on the C-line forming a visible red signal on the C-line. Hence, a positive result is obtained. Contradictorily, under the absence of the target, the labeled analyte will bind to both the T- and C-lines, resulting in two visible red lines, hence, portraying a negative result [56,57].

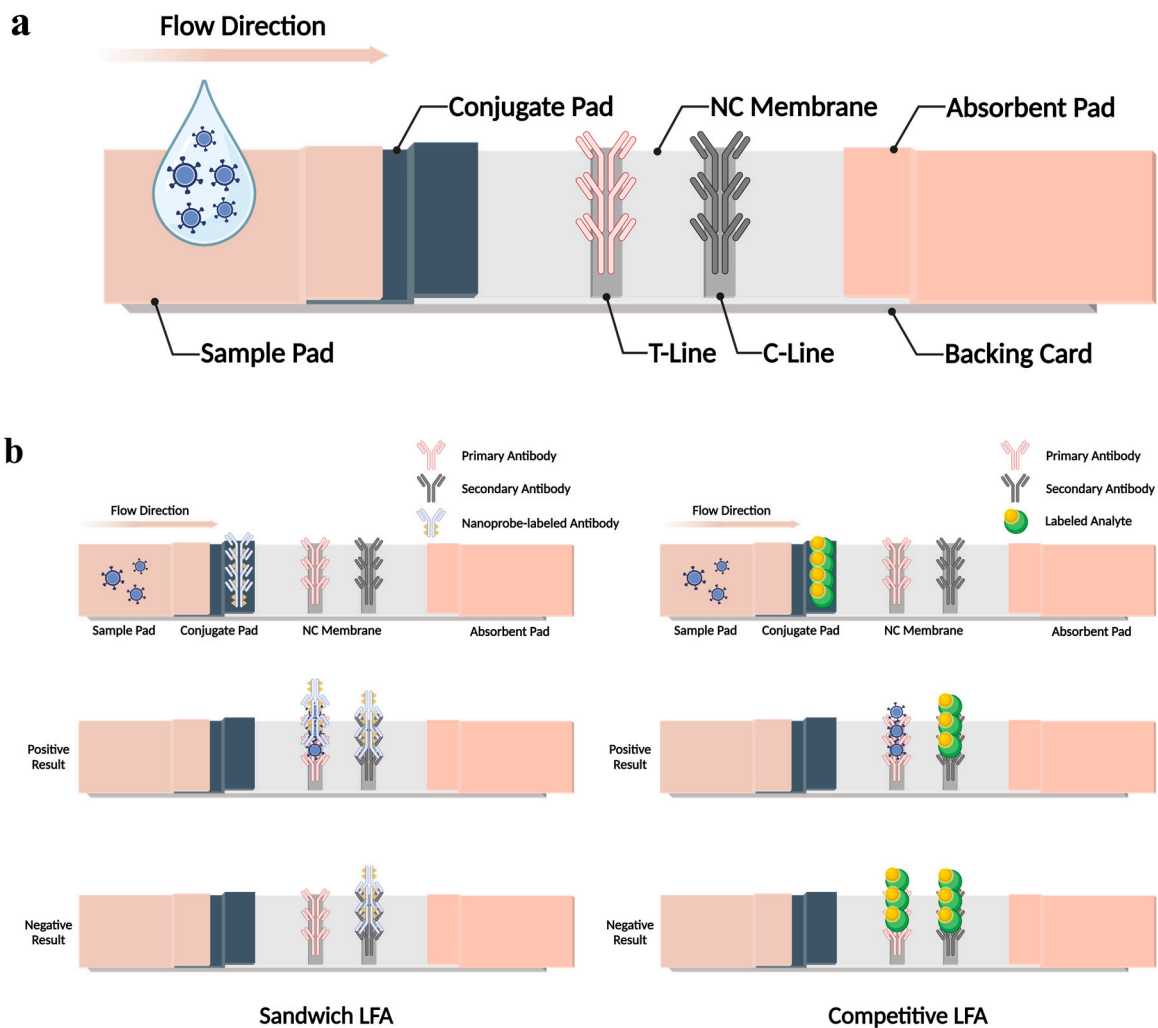


Figure 1. Components and structure of the LFA biosensor for viral protein detection. (a) Typical design of LFA strips with their components. (b) Widely utilized formats of LFA biosensors. Recreated with permission from [56]. Illustration designed with Biorender.com accessed on 10 March 2024.

In terms of nanomaterial-based LFA, the general principles are attained with only the addition of nanomaterials integrated in the system. In detail, various nanomaterials are used to aid in detection, especially for the signal amplification of optical sensing. The most commonly used nanomaterials are Au NPs. Au NPs can be synthesized in various sizes and shapes and produce a strong red color when viewed with the naked eye. Carbon-based materials, such as carbon nanoparticles, carbon nanotubes, etc., have been proposed as alternatives to Au NPs. Although this has a weak signal compared to Au NPs, it is stable and has significant cost advantages. In addition to this, dye-containing latex beads are inexpensive and resistant to chemical and physical damage. These nanomaterials also produce a weaker signal than Au NPs. Typically, QDs are the most commonly used in fluorescence-based LFAs and produce strong fluorescence signals through UV radiation. However, QDs have the disadvantages of being toxic and expensive. Upconversion nanoparticles (UCNPs) produce strong fluorescence signals in the near-infrared region; however, UCNPs are expensive and require NIR lasers. Liposomes are also used as nanomaterials for optical sensing. Liposomes are easy to use because they can encapsulate various nanomaterials, but they have the disadvantage of low stability due to their sensitivity to pH and ion strength [58]. In the subsequent chapter, we will present the latest studies on nanomaterial-based LFAs divided into three categories of optical sensing techniques: colorimetric, fluorescent, and SERS.

3. Colorimetric-Based LFAs for Viral Protein Detection

Au NPs are plasmon NPs commonly utilized as colorimetric diagnostic probes. Leveraging their inherent optical localized surface plasmon resonance (LSPR) and biocompatible properties, Au NPs are usually integrated into LFA systems. In detail, Au NPs are absorbed and scattered in the visible region, and they absorb millions of times more light than organic dye molecules due to their very high extinction coefficient ($\sim 10^9$ for 20 nm Au NPs) [59,60]. Thus, the conjugation of Au NPs with antibodies is a simple, fast, and reliable method for virus detection in the presence of a target virus on the T-line of an LFA system [59–61].

For this reason, many studies of colorimetric-based LFAs have reported the detection of viruses using Au NPs as nanoprobe [62–68]. For example, Shen et al. reported on a signal-enhanced LFA based on double Au NPs to determine hepatitis B surface antigens (HBsAgs). The Au NPs were modified with biotin and antibodies, Au NPs modified with streptavidin were used as conjugates, and the Au NPs were aggregated twice to improve the signal. When the sample solution flowed along the strip, the first conjugate was captured on the T-line by an antigen–antibody reaction, and the second conjugate was also immobilized on the T-line via biotin–streptavidin, resulting in a detection limit of 0.06 ng/mL HBsAgs [62]. To achieve the rapid diagnosis and field detection of IgM antibodies against the SARS-CoV-2 virus, Huang et al. coated SARS-CoV-2 nucleoprotein on an alkaline membrane, conjugated anti-human IgM with Au NPs to form a detection reporter, and constructed a colloidal Au NP-based LFA. Compared with real-time PCR, the sensitivity and specificity of Au NP-based LFAs are 100% and 93.3%, respectively (Figure 2a) [64]. Cavalera et al. designed a double-line LFA, which consists of recombinant SARS-CoV-2 nucleocapsid (N) protein and Au NPs as colorimetric signal reporters, and functions as a detector by indiscriminately binding to human Immunoglobulin G (IgG), Immunoglobulin M (IgM), and Immunoglobulin A (IgA). Both test lines comprised staphylococcal protein A (SpA) (T-line 1) and N antigen (T-line 2) [66]. The plasmon color-preserved (PLASCOP) Au NP clusters developed by Oh et al. were made by mixing a streptavidin-coated Au NP core with satellite Au NPs coated with biotinylated antibodies. The biotinylated antibody–streptavidin linker forms a gap of more than 15 nm to avoid plasmon bonding between the Au NPs, thus retaining the plasmon color while increasing the overall light absorption. LFA detection with PLASCOP Au NP clusters composed of 40 nm Au NPs had a limit of detection (LoD) of 0.038 ng/mL, indicating high detection sensitivity for the SARS-CoV-2 N protein [67].

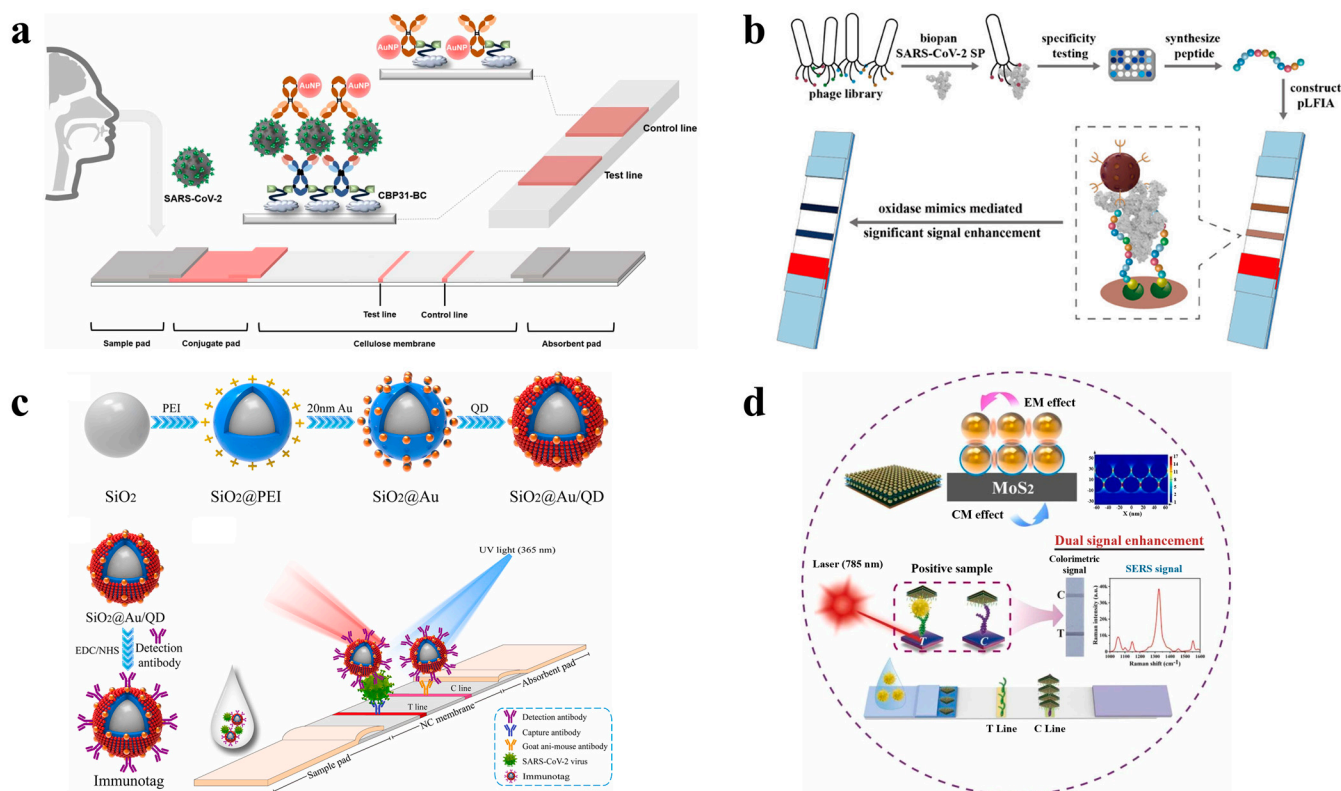


Figure 2. Examples of colorimetric-based LFAs for viral protein detection. (a) Scheme of the Au NP-based LFA for the detection of SARS-CoV-2. Reprinted in part with permission from ref. [64]. Copyright 2020 American Chemical Society. (b) Scheme of the polydopamine (PDA)@MnO₂ nanocomposite-based LFA for the detection of SARS-CoV-2. Reprinted in part with permission from ref. [69]. Copyright 2023 American Chemical Society. (c) Scheme of the SiO₂@Au/QD fluorescent labels of a dual-functional LFA for detecting SARS-CoV-2. Reprinted in part with permission from ref. [70]. Copyright 2022 Elsevier. (d) Scheme of the MoS₂@Au-Au-based LFA for the detection of the monkeypox virus (MPXV) antigen. Reprinted in part with permission from ref. [71]. Copyright 2023 Elsevier.

Enzyme signaling enhancement has traditionally been used for ELISA and colorimetric LFAs. Peroxidase enzymes have the advantages of being commercially available, stable, and inexpensive. The native peroxidase enzymes used in ELISA and other types of immunoassays are mainly horseradish peroxidase (HRP) and alkaline phosphatase (ALP) [72]. HRP is preferred for conjugation with LFA nanoprobe because it is stable, cost-effective, and easy to form into HRP-labeled antibodies/antigens for immunological recognition compared to other enzymes [73,74]. For example, an LFA platform has been proposed that can further amplify colorimetric signals by adding HRP to Fe₃O₄/Au core-shell magnetic NPs. The developed method detected 400 PFU/mL of SARS-CoV-2 in phosphate-buffered saline (PBS) buffer and detected 1200 PFU/mL of SARS-CoV-2 in saliva samples [75]. In addition, LFAs have also been proposed using a combination of Au NPs and ALPs for the high-sensitivity detection of virus X (PVX). Compared with natural enzymes, nanozymes have advantages such as low cost, high stability, and durability compared to natural enzymes [76]. For this reason, substances exhibiting peroxidase-mimicking activity (PMA) are sometimes employed as nanoprobe in LFAs [77,78]. Panferov et al. used Au@Pt core-shell NPs with PMA as probes, reducing the detection limits of PVX in tuber and leaf extracts to 4 and 8 pg/mL, respectively [79]. Sun et al. prepared LFAs enhanced by Au@Pd@Pt core-shell NPs to detect SARS-CoV-2 N proteins. Because Au@Pd@Pt nanozymes have good peroxidase-like activity due to their dendrite morphology and uniform particle size, they can generate catalytic signals even in small amounts [80]. Dong et al. used

PDA@MnO₂ nanocomposites with PMA as colorimetric labels, lowering the detection limit of SARS-CoV-2 spike antigens to 8.01 pg/mL (Figure 2b) [69].

Recently, dual detection methods have been developed to compensate for the sensitivity of colorimetric-based LFAs. Han et al. proposed a colorimetric and fluorescent dual-functional LFA that detects the spike 1 protein of SARS-CoV-2. For strong colorimetric and fluorescent signal generation, single dispersion, and high stability, a single-layer shell was formed by mixing 20 nm Au NPs with a SiO₂ core with QDs to generate a single-layer shell, resulting in a strong colorimetric and fluorescent signal and ensuring good monodispersity and high stability, thus creating a novel bifunctional immune marker. The colorimetric concentration of LoD is 1 ng/mL, and the fluorescence is 0.033 ng/mL (Figure 2c) [70]. Cheng et al. built a platform to simultaneously detect common respiratory viral influenza A and respiratory bacteria by forming a multi-layered double-signal nanofilm on a 16 nm layer, two layers of colorimetric Au NPs, and a QD monolayer graphene oxide (GO) surface [81]. Nanocomposites (MoS₂@Au-Au) adsorbed dense 30 nm Au NPs bilayers by coating a thickness-regulated polyethyleneimine intermediate layer (1 nm) on a two-dimensional molybdenum disulfide (MoS₂) nanosheet, which significantly enhanced the colorimetric capacity and SERS activity. Yu et al. showed that colorimetric signals supported the rapid identification of MPXV, and SERS signals enabled the quantitative detection of MPXV, with LoDs of 0.2 and 0.002 ng/mL (Figure 2d) [71]. Li et al. established a colorimetric and Raman bimodal LFA for the ultrasensitive detection of SARS-CoV-2 N proteins based on 4-mercaptobenzoic acid (MBA) Fe₃O₄-Ag^{MBA}@Au NPs with magnetic-Raman-colorimetric properties. Under optimal conditions, N protein antibodies could be detected qualitatively in colorimetric mode, with a visual limit of 10⁻⁸ mg/mL, and quantitatively by SERS signals between 10⁻⁶ and 10⁻¹⁰ mg/mL, with a detection limit of 0.08 pg/mL [82]. Wang et al. developed a colorimetric-fluorescent dual-mode LFA that simultaneously detects SARS-CoV-2-specific IgM and IgG in human serum. This proposal uses SiO₂@Au@QD nanobeads (NBs) as a label and has high enough sensitivity to require only one microliter of serum sample [83]. Liu et al. developed a colorimetric and fluorescent dual-functional LFA strip that introduced MXene and QDs to simultaneously detect IAV and SARS-CoV-2, which are difficult to distinguish due to their similar symptoms. High-sensitivity multiple detection of 1 ng/mL or 2.4 pg/mL IAV and 1 ng/mL or 6.2 pg/mL SARS-CoV-2 can be completed within 20 min [84]. Liang et al. prepared Ag NPs with ultrathin Au shells (~2 nm) embedded with MBA (Ag^{MBA}@Au) and incorporated them into LFAs for colorimetric and SERS bimodal detection of SARS-CoV-2 IgG. Qualitative analysis was performed through visual observation of the T-line, and quantitative analysis was performed by measuring the SERS signal [85]. A detailed list of colorimetric-based LFAs for viral protein detections is presented (Table 1).

Table 1. List of colorimetric-based LFAs for viral protein detection.

	Target	Nanoprobe	LoD	Reference
Au NP	HBsAg	Au NP	1.8 ng/mL	[62]
	Nodavirus	Au NP	6×10^{-3} TCID ₅₀	[63]
	SARS-CoV-2	PLASCOP Au NP cluster	0.038 ng/mL	[67]
	Japanese Encephalitis Virus	Au NP	10 pg/mL	[86]
	SARS-CoV-2	Au NP	0.2 mg/mL	[59]
	SARS-CoV-2	Au NP	5×10^4 copies/mL	[65]
Enzyme reaction	IAV, IBV	HRP	0.001~0.00025 HA units (IAV), 0.016~0.004 HA units (IBV)	[73]
	Dengue virus	HRP	5 ng/mL	[74]
	SARS-CoV-2	HRP-labeled Fe ₃ O ₄ /Au core-shell magnetic NP	400 PFU/mL	[75]
	PVX	ALP-labeled Au NP	0.3 ng/mL	[87]
	SARS-CoV-2	Au@Pd@Pt nanozyme	0.037 ng/mL	[80]

Table 1. Cont.

	Target	Nanoprobe	LoD	Reference
Enzyme reaction	SARS-CoV-2	ChF/ZnO/CNT nanohybrid	0.05 pg/mL	[88]
	SARS-CoV-2	PDA@MnO ₂ nanocomposite	8.01 pg/mL	[69]
Dual detection	SARS-CoV-2	SiO ₂ @Au NP/QD	1 ng/mL, 33 pg/mL (*C, F)	[70]
	IAV	GO-Au/QD-QD	5 × 10 ⁴ copies/mL, 891 copies/mL (*C, F)	[81]
	MPXV	MoS ₂ @Au–Au	0.2 ng/mL, 0.002 ng/mL (*C, S)	[71]
	SARS-CoV-2	Fe ₃ O ₄ -Ag ^{MBA} @Au NP	10 ⁻⁸ mg/mL, 0.08 pg/mL (*C, S)	[82]
	IAV, SARS-CoV-2	Ti ₃ C ₂ -QD	1 ng/mL, 2.4 pg/mL (IAV) 1 ng/mL, 6.2 pg/mL (SARS-CoV-2) (*C, F)	[84]
	SARS-CoV-2	Ag ^{MBA} @Au	10 ⁻⁶ mg/mL, 0.22 pg/mL (*C, S)	[85]
	SARS-CoV-2	Ag@Au triangular nanoplate	1 ng/mL, 40 pg/mL (*C, P)	[89]
SARS-CoV-2	Plasmonic-active Au nanocrown	91.24 pg/mL, 57.21 fg/mL (*C, S)	[90]	

*C: colorimetric signal, F: fluorescence signal, S: SERS signal, P: photothermal.

4. Fluorescence-Based LFAs for Viral Protein Detection

Fluorescence-based LFAs using QDs [68,91–95], fluorescent dye, and dye-doped NPs [96–100] as probes have been developed to improve analysis performance through strong fluorescence intensity [92,101]. For example, LFA, which detects anti-SARV-CoV-2 IgG in serum using lanthanide-doped polystyrene NPs (LNPs), achieves high sensitivity by labeling mouse anti-human IgG antibodies with self-assembled LNPs that act as fluorescent reporters [102]. Recently, for the detection of dengue fever (DF), a new diagnostic platform called spin-enhanced LFA (SELFIA) using fluorescent nanodiamonds (FNDs) as reporters has been reported. Leveraging the inherent magneto-optical properties of negatively charged nitrogen-vacancy centers in FNDs, the SELFIA platform utilizes alternating electromagnetic fields to modulate signals from the fluorescence of FNDs, providing sensitive and specific results. This enabled us to efficiently detect all four dengue non-structural protein (NS1) serotypes (DV1, DV2, DV3, and DV4) [103].

A metal-enhanced fluorescence (MEF) probe based on core-shell nanostructures using a gold nanorod core, mesoporous silica shell, and cyanine 5 (Cy5) fluorophore has also been designed. In this study, the distance dependence of plasma coupling between Cy5 and gold nanorods was experimentally and theoretically investigated by adjusting the shell thickness to optimize the efficiency of the MEF probe, which significantly improved fluorescence. This platform enabled the high-sensitivity detection of the IAV N protein with an LoD of 0.52 pg/mL within 20 min (Figure 3b) [104].

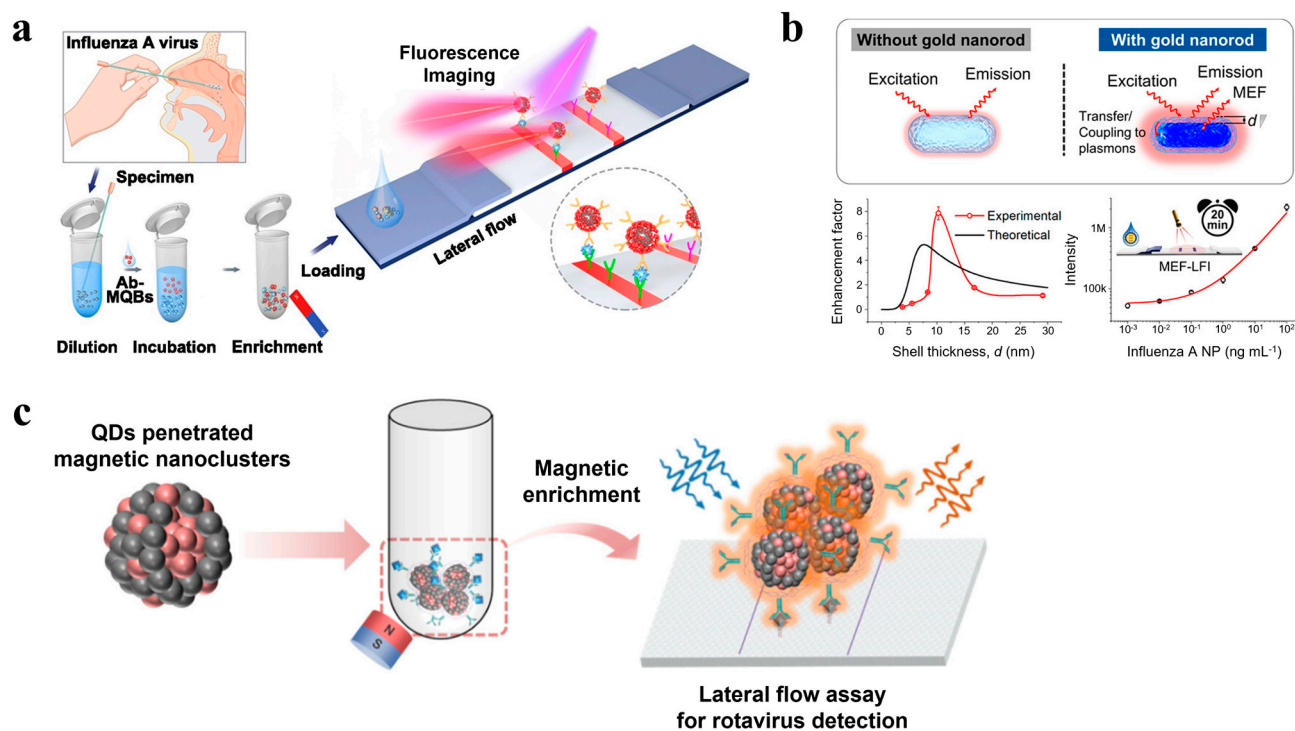


Figure 3. Examples of fluorescence-based LFAs for viral protein detection. (a) Scheme of the Magnetic-QD NB-based LFA for the detection of IAV. Reprinted in part with permission from ref. [95]. Copyright 2020 Elsevier. (b) Scheme of the mesoporous silica-coated gold nanorod-based LFA for the detection of IAV. Reprinted in part with permission from ref. [104]. Copyright 2023 American Chemical Society. (c) Scheme of the magnetic–fluorescent nanocluster composed of Fe₃O₄ NPs and CdSe–CdS core–shell QD-based LFA for the detection of rotavirus. Reprinted in part with permission from ref. [105]. Copyright 2023 American Chemical Society.

Although there are a variety of fluorescent reporters, QDs have several prominent features, such as high quantum yields, wide excitation, and narrow, size-adjustable fluorescence emission spectra, which are widely used in fluorescent LFAs [101,106]. Wang et al. developed a magnetic-QD-based dual-mode LFA for the simultaneous high-sensitivity detection of SARS-CoV-2 spike (S) and N protein antigens. A high-performance magnetic QD with a triple-QD shell (MagTQD) nanotag was used to provide excellent fluorescence signals, enrichment capabilities, and detection potential. The LoDs for the two antigens under direct and enrichment modes were 1 and 0.5 pg/mL, respectively [107]. Li et al. designed an LFA to rapidly detect SARS-CoV-2-specific antibodies using ZnCdSe/ZnS QDs as probes. The LoD of IgG was 48.84 ng/mL [108]. For the multiple detection of four respiratory viruses, a QD NB-based LFA was presented by Chen and their research group. The sandwich complex formed by the detection antibody on the QDs' surface and the capture antibody on the T-line was excited by ultraviolet light, emitting a red fluorescence signal at a specific wavelength. Their study achieved excellent LoDs of 0.01 ng/mL, 0.05 ng/mL, 0.31 ng/mL, and 0.40 ng/mL for the SARS-CoV-2 antigen, IAV antigen, IBV antigen, and adenovirus (ADV) antigen, respectively [109]. Researchers constructed magnetic–fluorescent CdSe–CdS (QD)/Fe₃O₄ nanoclusters (CFNCs) consisting of magnetic NPs and CdSe–CdS core–shells for detecting rotaviruses. QDs are embedded in the inner and outer shells of Fe₃O₄ NCs, which can weaken the solubility interactions mediated by solvent polarity, and by increasing the particle-to-particle distances, the CFNCs can overcome the fluorescence quenching effect. The LoD was improved to 1.0×10^1 TCID₅₀/mL, and high sensitivity was achieved (Figure 3c) [105]. A detailed list of fluorescence-based LFAs for viral protein detections is tabulated (Table 2).

Table 2. List of fluorescence-based LFAs for viral protein detection.

	Target	Nanoprobe	LoD	Reference
Fluorophore	SARS-CoV-2	Fluorescent microsphere	100 ng/mL	[98]
	SARS-CoV-2	Aggregation-induced emission ₈₁₀ NP	0.236 µg/mL (IgM), 0.125 µg/mL (IgG)	[97]
	Dengue NS1 serotypes (DV1, DV2, DV3, DV4)	FND	0.33, 0.24, 0.10, 1.33 ng/mL	[103]
	IAV	Cy5-mSiO ₂ @GNR	0.52 pg /mL	[104]
	SARS-CoV-2	Fluorescent microsphere	0.01 ng/mL	[105]
QD	Zika virus	QD microsphere	0.045 ng/mL	[68]
	Thrombocytopenia syndrome virus	Fluorescent carbon dots (CDs)/SiO ₂ nanosphere	10 pg/mL	[91]
	IAV	CdSe/CdS/ZnS QD	2.5 HAU/mL (H1N1), 0.63 HAU/mL (H3N2)	[93]
	Zika virus	Fluorescent CD-based silica colloid	10 pg/mL	[94]
	IAV	Magnetic-QD NB	22 pfu/mL	[95]
	SARS-CoV-2	MagTQD	0.5 pg/mL	[107]
	SARS-CoV-2, IAV, IBV, ADV	QD NB	0.01, 0.05, 0.31, 0.40 ng/mL	[109]
	Rotavirus	CFNC	1.0 × 10 ¹ TCID ₅₀ /mL	[105]

5. SERS-Based LFAs for Viral Protein Detection

Based on LSPR excitation, SERS can enhance the Raman signaling of targets adsorbed by Au or Ag metal nanomaterials by several orders of magnitude. For an LFA system using NIR dye-labeled Au NPs as probes, the LoD of SARS-CoV-2-specific IgM/IgG was 100 fg/mL [110]. The LoDs of SARS-CoV-2 and IAV were 5.2 PFU/mL and 23 HAU/mL, respectively, in an LFA platform constructed by attaching malachite green isothiocyanate (MGITC) to Au NPs [111]. However, Raman reporter molecules may dissociate from the surface of Au NPs when exposed to high temperatures, harsh pH, or salty conditions [112]. To address this issue, silica-encapsulated metal NPs have been developed to prevent the desorption of Raman reporter molecules and the adsorption of external species of molecules [113,114]. For this reason, a platform has been reported that can apply silica-encapsulated metal NPs to LFA strips to minimize changes in SERS intensity and maintain stability even under high-temperature conditions (Figure 4) [115,116]. Furthermore, to overcome the limitations of single metals, hybrid fabrication methods for metal cores and metal shells have been developed, such as uniformly coating the Ag core with an ultrathin film of Au to functionalize the surface chemistry of Au and the optical properties of Ag to the probe itself [117–119]. This structure enhances the SERS signal via the SERS-enhancing effect of precious metals, large numbers of Raman molecules, and the hotspot effect in the narrow gap between metal cores and metal shells [117]. Metal shells aid in binding to biomolecules, protecting the inner metal core and keeping Raman reporter molecules unaffected by outside conditions, thereby enhancing the biocompatibility and the chemical and signal stability of the particles [85]. Liang et al. developed a SERS/photothermal (PT)-based dual-mode LFA based on Au-core–Ag-shell bimetallic NPs (Au^{4-ATP}@Ag NPs) for the antigen detection of infectious disease pathogens. The quantified LoDs for IAV, influenza B virus (IBV), and SARS-CoV-2 were 31.25 pg/mL, 93.75 pg/mL, and 31.25 pg/mL, respectively [119]. Recently, researchers have developed an ultralight SERS probe [120–122] by coating an Au core and Ag shell NPs (Au@Ag NPs) with an Au layer and encapsulating Raman molecules between them, in which the Raman reporter between the core and shell has an intense electromagnetic field enhancement effect, which significantly boosts the Raman signals in virus detection [123,124].

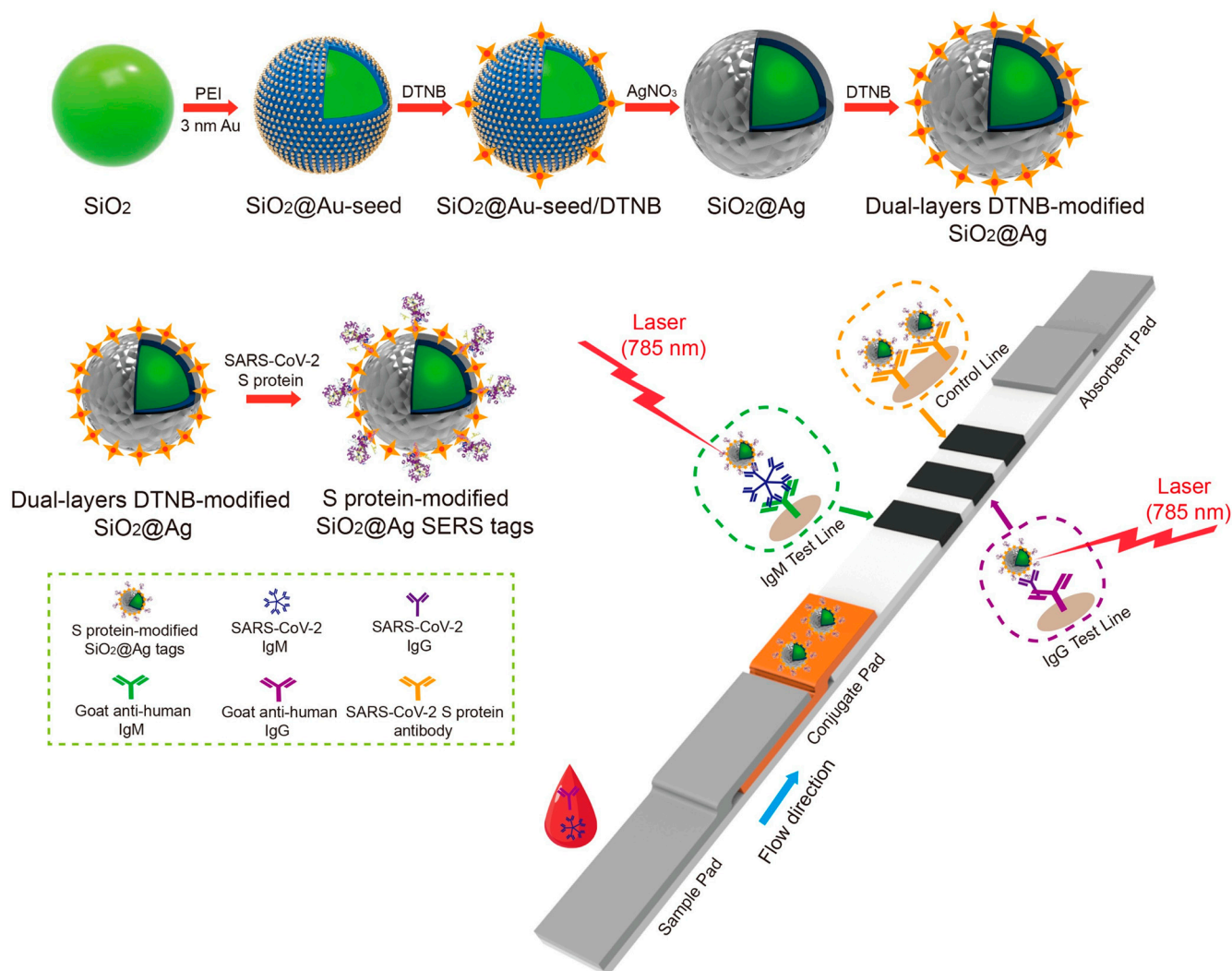


Figure 4. A SERS-based LFA for viral protein detection. Scheme of the dual layer DTNB-modified $\text{SiO}_2@\text{Ag}$ SERS tag-based LFA detecting SARS-CoV-2. Reprinted in part with permission from ref. [116]. Copyright 2021 Elsevier.

Magnetic SERS tags can be used as stable SERS tags for separating target analytes from complex solutions by using external magnetic fields and improving the Raman signal of the target [125–127]. LFAs that simultaneously detect IAV H1N1 and human ADV using $\text{Fe}_3\text{O}_4@\text{Ag}$ NPs as magnetic SERS nanotags have been reported. A new type of $\text{Fe}_3\text{O}_4@\text{Ag}$ magnetic tag combined with a bilayer Raman dye molecule and a target virus-capture antibody allows for the specific recognition of the target virus in solution and SERS detection of the virus via magnetic enrichment and strips. The LoDs of H1N1 and human ADV were 50 pfu/mL and 10 pfu/mL, respectively, making this method 2000 times more sensitive than the standard colloidal Au strip method [128]. For the rapid and accurate measurement of SARS-CoV-2 N proteins, a novel multifunctional NB-based magnetic/fluorescent dual-mode LFA was developed by combining a superparamagnetic Fe_3O_4 core with double quantum dot shells (MagDQDs) using polyethyleneimine (PEI) as the carrier shell. Both the magnetic and fluorescent signals showed high sensitivity with LoDs of 0.235 ng/mL and 0.012 ng/mL, respectively [129]. A SERS LFA system based on $\text{Fe}_3\text{O}_4@\text{Au}$ magnetic NPs for the simultaneous and supersensitive detection of three respiratory viruses (H1N1/SARS-CoV-2/RSV) has been proposed. 5,5'-Dithiobis-(2-nitrobenzoic acid) (DTNB) was modified from $\text{Fe}_3\text{O}_4@\text{Au}$ magnetic NPs to prepare a magnetic SERS tag, providing abundant binding sites for high SERS signals and antibodies. The concentrations of LoD were 85 copies/mL, 8 pg/mL, and 8 pg/mL for H1N1, SARS-

CoV-2 and RSV, respectively [130]. A detailed list of SERS-based LFAs for viral protein detection is presented (Table 3).

Table 3. List of SERS-based LFAs for viral protein detection.

	Target	Nanoprobe	LoD	Reference
Noble metal	Pseudorabies virus	AuAg ^{4−ATP} @Ag NP	5 ng/mL	[120]
	Avian influenza virus	AuAg ^{4−ATP} @Ag NP	0.0018 HAU	[121]
	Dengue virus, Zika virus	MGITC-labeled Si-Au NP	1.906 µg/mL	[115]
	SARS-CoV-2	dual-layer DTNB-modified SiO ₂ @Ag NP	1 pg/mL	[116]
	Rotavirus	Au/DTNB/Ag/DTNB	8 pg/mL	[117]
	West Nile virus	Au@Ag NP	0.2 × 10 ² copy/µL	[118]
	SARS-CoV-2	NIR-797-ITC-labeled Au nanostar	100 fg/mL	[110]
	SARS-CoV-2, IAV	MGITC-labeled Au NP	5.2 PFU/mL (SARS-CoV-2), 23 HAU/mL (IAV)	[111]
Magnetic NP	IAV, human ADV	Fe ₃ O ₄ @Ag magnetic tag	50 pfu/mL, 10 pfu/mL	[128]
	SARS-CoV-2	MagDQD	0.235 ng/mL, 0.012 ng/mL (*M, F)	[129]
	IAV, SARS-CoV-2, respiratory syncytial virus	Fe ₃ O ₄ /DTNB@Au/DTNB	85 copies/mL, 8 pg/mL, 8 pg/mL	[130]
	SARS-CoV-2	DTNB-encoded satellite Fe ₃ O ₄ @Au SERS tag	23 pg/mL, 2 pg/mL	[131]

*M: magnetic signal, F: fluorescence signal.

6. Conclusions

This review identified and discussed the principles, mechanisms, and research trends of LFA-based analyses for viral protein detection. Since viral infectious diseases occur and spread worldwide and have a significant influence on human life, accurate and highly sensitive methods for quickly diagnosing infectious diseases and controlling their spread are essential. Thus, we believe that using LFA platforms can be an appropriate method because they have the advantages of significant cost benefits, simple analysis with minimal training or infrastructure, and a short diagnosis time.

Briefly, LFAs can generally be classified based on the detection method. Au NPs are most often used in colorimetric LFAs. The sensitivity is increased through a double detection mode in which peroxidase enzyme activity is used or colorimetric detection is integrated with detection methods such as fluorescence or SERS. For example, fluorescent LFAs using QDs, fluorescent dyes, and dye-doped NPs as probes improve analysis performance through strong fluorescence intensity. Finally, based on the excitation of LSPR, SERS LFAs can improve the Raman signal of the target adsorbed on the precious metal nanostructure by several times. Recently, to maximize SERS intensity and maintain stability even under high-temperature conditions, silica-encapsulated metal NPs and core-shell structures composed of precious metals have been used as probes.

Despite the steady progress of research on LFA systems, developing a simple and stable LFA system capable of exhibiting high selectivity and sensitivity is still a major and fundamental task. Throughout the course of a viral infectious disease, protein levels tend to increase towards the end of the infection, whereas nucleic acid levels are typically higher at the beginning. Based on the literature that we compiled, the idea of integrating the current approaches for the individual detection of proteins and nucleic acids into a unified LFA system capable of simultaneously identifying both components makes it feasible to consistently achieve high-sensitivity detection outcomes throughout the infection period. Additionally, in recent times, the method of multiplexing capabilities for biomarker detection has also actively flourished within the scientific field [132]. In addition to this, trends such as the development of equipment-free signal readout for semi-quantitative and quantitative analysis have been gaining attention due to its indispensable increased

usability and accessibility within paper-based sensors, especially the LFA system [133]. As an example, the conventional qualitative detection output of yes/no has been transformed into measurements based on color distance, counts of area color changes, text readout displays, and other technologies [134–136]. In detail, this concise review on the trend of transformation was put together based on a review paper by a group of researchers on papers published from 2020 to 2023 [137]. In conclusion, the integration of nanomaterials in LFA systems can be expected to detect viral proteins in clinical diagnosis, and to be used in various fields, such as environmental protection.

Author Contributions: J.-H.C., M.J.K. and M.J.A. organized the structure of the manuscript. M.J.K. and I.H. wrote the whole manuscript. J.-H.C., M.J.K., I.H. and D.-H.P. revised the manuscript. All authors collaboratively wrote the manuscript. All authors have read and agreed to the published version of the manuscript.

Funding: This work was supported by a National Research Foundation of Korea (NRF) grant funded by the Korean government (MSIT) (NRF-2022R1C1C1008797); by the Bio & Medical Technology Development Program of the National Research Foundation (NRF) funded by the Korean government (MSIT) (No. RS-2023-00236157); and by grants from the Biomedical Research Institute of Jeonbuk National University Hospital, Jeonju, Korea.

Institutional Review Board Statement: Not applicable.

Informed Consent Statement: Not applicable.

Data Availability Statement: Not applicable.

Conflicts of Interest: The authors declare no conflicts of interest.

References

1. Dance, A. Beyond Coronavirus: The Virus Discoveries Transforming Biology. *Nature* **2021**, *595*, 22–25. [[CrossRef](#)]
2. Dronina, J.; Samukaite-Bubniene, U.; Ramanavicius, A. Towards Application of CRISPR-Cas12a in the Design of Modern Viral DNA Detection Tools (Review). *J. Nanobiotechnol.* **2022**, *20*, 41. [[CrossRef](#)]
3. Baker, R.E.; Mahmud, A.S.; Miller, I.F.; Rajeev, M.; Rasambainarivo, F.; Rice, B.L.; Takahashi, S.; Tatem, A.J.; Wagner, C.E.; Wang, L.-F.; et al. Infectious Disease in an Era of Global Change. *Nat. Rev. Microbiol.* **2022**, *20*, 193–205. [[CrossRef](#)] [[PubMed](#)]
4. Ka-Wai Hui, E. Reasons for the Increase in Emerging and Re-Emerging Viral Infectious Diseases. *Microbes Infect.* **2006**, *8*, 905–916. [[CrossRef](#)]
5. Edelson, P.J.; Harold, R.; Ackelsberg, J.; Duchin, J.S.; Lawrence, S.J.; Manabe, Y.C.; Zahn, M.; LaRocque, R.C. Climate Change and the Epidemiology of Infectious Diseases in the United States. *Clin. Infect. Dis.* **2023**, *76*, 950–956. [[CrossRef](#)]
6. Russell, R.C. Survival of Insects in the Wheel Bays of a Boeing 747B Aircraft on Flights between Tropical and Temperate Airports. *Bull. World Health Organ.* **1987**, *65*, 659–662. [[PubMed](#)]
7. Roberts, J.D.; Tehrani, S.O. Environments, Behaviors, and Inequalities: Reflecting on the Impacts of the Influenza and Coronavirus Pandemics in the United States. *Int. J. Environ. Res. Public Health* **2020**, *17*, 4484. [[CrossRef](#)] [[PubMed](#)]
8. Flerlage, T.; Boyd, D.F.; Meliopoulos, V.; Thomas, P.G.; Schultz-Cherry, S. Influenza Virus and SARS-CoV-2: Pathogenesis and Host Responses in the Respiratory Tract. *Nat. Rev. Microbiol.* **2021**, *19*, 425–441. [[CrossRef](#)]
9. Drosten, C.; Günther, S.; Preiser, W.; van der Werf, S.; Brodt, H.-R.; Becker, S.; Rabenau, H.; Panning, M.; Kolesnikova, L.; Fouchier, R.A.M.; et al. Identification of a Novel Coronavirus in Patients with Severe Acute Respiratory Syndrome. *N. Engl. J. Med.* **2003**, *348*, 1967–1976. [[CrossRef](#)]
10. Cauchemez, S.; Fraser, C.; Van Kerkhove, M.D.; Donnelly, C.A.; Riley, S.; Rambaut, A.; Enouf, V.; van der Werf, S.; Ferguson, N.M. Middle East Respiratory Syndrome Coronavirus: Quantification of the Extent of the Epidemic, Surveillance Biases, and Transmissibility. *Lancet Infect. Dis.* **2014**, *14*, 50–56. [[CrossRef](#)]
11. de Wit, E.; van Doremalen, N.; Falzarano, D.; Munster, V.J. SARS and MERS: Recent Insights into Emerging Coronaviruses. *Nat. Rev. Microbiol.* **2016**, *14*, 523–534. [[CrossRef](#)] [[PubMed](#)]
12. Mofijur, M.; Fattah, I.M.R.; Alam, M.A.; Islam, A.B.M.S.; Ong, H.C.; Rahman, S.M.A.; Najafi, G.; Ahmed, S.F.; Uddin, M.d.A.; Mahlia, T.M.I. Impact of COVID-19 on the Social, Economic, Environmental and Energy Domains: Lessons Learnt from a Global Pandemic. *Sustain. Prod. Consum.* **2021**, *26*, 343–359. [[CrossRef](#)] [[PubMed](#)]
13. Hou, Y.J.; Okuda, K.; Edwards, C.E.; Martinez, D.R.; Asakura, T.; Dinnon, K.H.; Kato, T.; Lee, R.E.; Yount, B.L.; Mascenik, T.M.; et al. SARS-CoV-2 Reverse Genetics Reveals a Variable Infection Gradient in the Respiratory Tract. *Cell* **2020**, *182*, 429–446.e14. [[CrossRef](#)] [[PubMed](#)]
14. Chakraborty, I.; Maity, P. COVID-19 Outbreak: Migration, Effects on Society, Global Environment and Prevention. *Sci. Total Environ.* **2020**, *728*, 138882. [[CrossRef](#)]

15. Piot, P.; Bartos, M.; Ghys, P.; Walker, N.; Schwartländer, B. The Global Impact of HIV/AIDS. *Nature* **2001**, *410*, 968–973. [[CrossRef](#)] [[PubMed](#)]
16. Omoleke, S.A.; Mohammed, I.; Saidu, Y. Ebola Viral Disease in West Africa: A Threat to Global Health, Economy and Political Stability. *J. Public Health Afr.* **2016**, *7*, 534. [[CrossRef](#)] [[PubMed](#)]
17. de Graaf, M.; van Beek, J.; Koopmans, M.P.G. Human Norovirus Transmission and Evolution in a Changing World. *Nat. Rev. Microbiol.* **2016**, *14*, 421–433. [[CrossRef](#)] [[PubMed](#)]
18. Nikookar, S.H.; Fazeli-Dinan, M.; Enayati, A.; Zaim, M. Zika; a Continuous Global Threat to Public Health. *Environ. Res.* **2020**, *188*, 109868. [[CrossRef](#)] [[PubMed](#)]
19. Sharma, A.; Ghosh, D.; Divekar, N.; Gore, M.; Gochhait, S.; Shireshi, S.S. Comparing the Socio-economic Implications of the 1918 Spanish Flu and the COVID-19 Pandemic in India: A Systematic Review of Literature. *Int. Soc. Sci. J.* **2021**, *71*, 23–36. [[CrossRef](#)]
20. Carter, L.J.; Garner, L.V.; Smoot, J.W.; Li, Y.; Zhou, Q.; Saveson, C.J.; Sasso, J.M.; Gregg, A.C.; Soares, D.J.; Beskid, T.R.; et al. Assay Techniques and Test Development for COVID-19 Diagnosis. *ACS Cent. Sci.* **2020**, *6*, 591–605. [[CrossRef](#)]
21. Shen, M.; Zhou, Y.; Ye, J.; Abdullah AL-Maskri, A.A.; Kang, Y.; Zeng, S.; Cai, S. Recent Advances and Perspectives of Nucleic Acid Detection for Coronavirus. *J. Pharm. Anal.* **2020**, *10*, 97–101. [[CrossRef](#)] [[PubMed](#)]
22. Shafie, M.H.; Antony Dass, M.; Ahmad Shaberi, H.S.; Zafarina, Z. Screening and Confirmation Tests for SARS-CoV-2: Benefits and Drawbacks. *Beni-Suef Univ. J. Basic Appl. Sci.* **2023**, *12*, 6. [[CrossRef](#)] [[PubMed](#)]
23. Xu, M.; Wang, D.; Wang, H.; Zhang, X.; Liang, T.; Dai, J.; Li, M.; Zhang, J.; Zhang, K.; Xu, D.; et al. COVID-19 Diagnostic Testing: Technology Perspective. *Clin. Transl. Med.* **2020**, *10*, e158. [[CrossRef](#)] [[PubMed](#)]
24. Shahrajabian, M.H.; Sun, W. Various Techniques for Molecular and Rapid Detection of Infectious and Epidemic Diseases. *Lett. Org. Chem.* **2023**, *20*, 779–801. [[CrossRef](#)]
25. Tahamtan, A.; Ardebili, A. Real-Time RT-PCR in COVID-19 Detection: Issues Affecting the Results. *Expert Rev. Mol. Diagn.* **2020**, *20*, 453–454. [[CrossRef](#)] [[PubMed](#)]
26. Liu, R.; Fu, A.; Deng, Z.; Li, Y.; Liu, T. Promising Methods for Detection of Novel Coronavirus SARS-CoV-2. *View* **2020**, *1*, e4. [[CrossRef](#)] [[PubMed](#)]
27. Corman, V.M.; Landt, O.; Kaiser, M.; Molenkamp, R.; Meijer, A.; Chu, D.K.; Bleicker, T.; Brünink, S.; Schneider, J.; Schmidt, M.L.; et al. Detection of 2019 Novel Coronavirus (2019-NCoV) by Real-Time RT-PCR. *Eurosurveillance* **2020**, *25*, 2000045. [[CrossRef](#)] [[PubMed](#)]
28. Li, C.; Debruyne, D.N.; Spencer, J.; Kapoor, V.; Liu, L.Y.; Zhou, B.; Pandey, U.; Bootwalla, M.; Ostrow, D.; Maglinte, D.T.; et al. Highly Sensitive and Full-Genome Interrogation of SARS-CoV-2 Using Multiplexed PCR Enrichment Followed by next-Generation Sequencing. *bioRxiv* 2020. [[CrossRef](#)]
29. Kurosaki, Y.; Martins, D.B.G.; Kimura, M.; Catena, A.d.S.; Borba, M.A.C.S.M.; Mattos, S.d.S.; Abe, H.; Yoshikawa, R.; de Lima Filho, J.L.; Yasuda, J. Development and Evaluation of a Rapid Molecular Diagnostic Test for Zika Virus Infection by Reverse Transcription Loop-Mediated Isothermal Amplification. *Sci. Rep.* **2017**, *7*, 13503. [[CrossRef](#)]
30. Shirato, K.; Yano, T.; Senba, S.; Akachi, S.; Kobayashi, T.; Nishinaka, T.; Notomi, T.; Matsuyama, S. Detection of Middle East Respiratory Syndrome Coronavirus Using Reverse Transcription Loop-Mediated Isothermal Amplification (RT-LAMP). *Virol. J.* **2014**, *11*, 139. [[CrossRef](#)]
31. Shirato, K.; Semba, S.; El-Kafrawy, S.A.; Hassan, A.M.; Tolah, A.M.; Takayama, I.; Kageyama, T.; Notomi, T.; Kamitani, W.; Matsuyama, S.; et al. Development of Fluorescent Reverse Transcription Loop-Mediated Isothermal Amplification (RT-LAMP) Using Quenching Probes for the Detection of the Middle East Respiratory Syndrome Coronavirus. *J. Virol. Methods* **2018**, *258*, 41–48. [[CrossRef](#)] [[PubMed](#)]
32. Choi, S.; Goryll, M.; Sin, L.Y.M.; Wong, P.K.; Chae, J. Microfluidic-Based Biosensors toward Point-of-Care Detection of Nucleic Acids and Proteins. *Microfluid. Nanofluidics* **2011**, *10*, 231–247. [[CrossRef](#)]
33. Aydin, S. A Short History, Principles, and Types of ELISA, and Our Laboratory Experience with Peptide/Protein Analyses Using ELISA. *Peptides* **2015**, *72*, 4–15. [[CrossRef](#)] [[PubMed](#)]
34. Wu, L.; Li, G.; Xu, X.; Zhu, L.; Huang, R.; Chen, X. Application of Nano-ELISA in Food Analysis: Recent Advances and Challenges. *TrAC Trends Anal. Chem.* **2019**, *113*, 140–156. [[CrossRef](#)]
35. Mohit, E.; Rostami, Z.; Vahidi, H. A Comparative Review of Immunoassays for COVID-19 Detection. *Expert Rev. Clin. Immunol.* **2021**, *17*, 573–599. [[CrossRef](#)] [[PubMed](#)]
36. Stadlbauer, D.; Amanat, F.; Chromikova, V.; Jiang, K.; Strohmeier, S.; Arunkumar, G.A.; Tan, J.; Bhavsar, D.; Capuano, C.; Kirkpatrick, E.; et al. SARS-CoV-2 Seroconversion in Humans: A Detailed Protocol for a Serological Assay, Antigen Production, and Test Setup. *Curr. Protoc. Microbiol.* **2020**, *57*, e100. [[CrossRef](#)] [[PubMed](#)]
37. Krähling, V.; Halwe, S.; Rohde, C.; Becker, D.; Berghöfer, S.; Dahlke, C.; Eickmann, M.; Ercanoglu, M.S.; Gieselmann, L.; Herwig, A.; et al. Development and Characterization of an Indirect ELISA to Detect SARS-CoV-2 Spike Protein-Specific Antibodies. *J. Immunol. Methods* **2021**, *490*, 112958. [[CrossRef](#)]
38. Urusov, A.E.; Zherdev, A.V.; Dzantiev, B.B. Towards Lateral Flow Quantitative Assays: Detection Approaches. *Biosensors* **2019**, *9*, 89. [[CrossRef](#)]
39. Andryukov, B.G. Six Decades of Lateral Flow Immunoassay: From Determining Metabolic Markers to Diagnosing COVID-19. *AIMS Microbiol.* **2020**, *6*, 280–304. [[CrossRef](#)]

40. Pilavaki, E.; Demosthenous, A. Optimized Lateral Flow Immunoassay Reader for the Detection of Infectious Diseases in Developing Countries. *Sensors* **2017**, *17*, 2673. [[CrossRef](#)]
41. Banerjee, R.; Jaiswal, A. Recent Advances in Nanoparticle-Based Lateral Flow Immunoassay as a Point-of-Care Diagnostic Tool for Infectious Agents and Diseases. *Analyst* **2018**, *143*, 1970–1996. [[CrossRef](#)] [[PubMed](#)]
42. Grant, B.D.; Anderson, C.E.; Alonzo, L.F.; Garing, S.H.; Williford, J.R.; Baughman, T.A.; Rivera, R.; Glukhova, V.A.; Boyle, D.S.; Dewan, P.K.; et al. A SARS-CoV-2 Coronavirus Nucleocapsid Protein Antigen-Detecting Lateral Flow Assay. *PLoS ONE* **2021**, *16*, e0258819. [[CrossRef](#)] [[PubMed](#)]
43. Kim, K.; Kim, M.-J.; Kim, D.W.; Kim, S.Y.; Park, S.; Park, C.B. Clinically Accurate Diagnosis of Alzheimer’s Disease via Multiplexed Sensing of Core Biomarkers in Human Plasma. *Nat. Commun.* **2020**, *11*, 119. [[CrossRef](#)] [[PubMed](#)]
44. Borrebaeck, C.A.K. Precision Diagnostics: Moving towards Protein Biomarker Signatures of Clinical Utility in Cancer. *Nat. Rev. Cancer* **2017**, *17*, 199–204. [[CrossRef](#)] [[PubMed](#)]
45. Jin, Z.; Mantri, Y.; Retout, M.; Cheng, Y.; Zhou, J.; Jorns, A.; Fajtova, P.; Yim, W.; Moore, C.; Xu, M.; et al. A Charge-Switchable Zwitterionic Peptide for Rapid Detection of SARS-CoV-2 Main Protease. *Angew. Chem.* **2022**, *134*, e202112995. [[CrossRef](#)]
46. Harshita; Wu, H.F.; Kailasa, S.K. Recent Advances in Nanomaterials-based Optical Sensors for Detection of Various Biomarkers (Inorganic Species, Organic and Biomolecules). *Luminescence* **2022**, *38*, 954–998. [[CrossRef](#)] [[PubMed](#)]
47. Singh, H.; Bamrah, A.; Bhardwaj, S.K.; Deep, A.; Khatri, M.; Kim, K.-H.; Bhardwaj, N. Nanomaterial-Based Fluorescent Sensors for the Detection of Lead Ions. *J. Hazard. Mater.* **2021**, *407*, 124379. [[CrossRef](#)] [[PubMed](#)]
48. Bhardwaj, N.; Bhardwaj, S.K.; Bhatt, D.; Lim, D.K.; Kim, K.-H.; Deep, A. Optical Detection of Waterborne Pathogens Using Nanomaterials. *TrAC Trends Anal. Chem.* **2019**, *113*, 280–300. [[CrossRef](#)]
49. Qiu, S.; Zhang, H.; Shi, Z.; Li, H.; Zhou, Z.-K. Ultrasensitive Refractive Index Sensing Based on Hybrid High-Q Metasurfaces. *J. Phys. Chem. C* **2023**, *127*, 8263–8270. [[CrossRef](#)]
50. Zhang, L.; Fu, Q.; Tan, Y.; Li, X.; Deng, Y.; Zhou, Z.-K.; Zhou, B.; Xia, H.; Chen, H.; Qiu, C.-W.; et al. Metaoptronic Multiplexed Interface for Probing Bioentity Behaviors. *Nano Lett.* **2021**, *21*, 2681–2689. [[CrossRef](#)]
51. O’Farrell, B. Evolution in Lateral Flow–Based Immunoassay Systems. In *Lateral Flow Immunoassay*; Humana Press: Totowa, NJ, USA, 2009; pp. 1–33.
52. Asghari, S.; Ekrami, E.; Barati, F.; Avatefi, M.; Mahmoudifard, M. The Role of the Nanofibers in Lateral Flow Assays Enhancement: A Critical Review. *Int. J. Polym. Mater. Polym. Biomater.* **2023**, *72*, 1191–1204. [[CrossRef](#)]
53. Tsai, T.-T.; Huang, T.-H.; Chen, C.-A.; Ho, N.Y.-J.; Chou, Y.-J.; Chen, C.-F. Development a Stacking Pad Design for Enhancing the Sensitivity of Lateral Flow Immunoassay. *Sci. Rep.* **2018**, *8*, 17319. [[CrossRef](#)] [[PubMed](#)]
54. Dowlatshahi, S.; Shabani, E.; Abdekhodaie, M.J. Serological Assays and Host Antibody Detection in Coronavirus-Related Disease Diagnosis. *Arch. Virol.* **2021**, *166*, 715–731. [[CrossRef](#)] [[PubMed](#)]
55. Mak, W.C.; Beni, V.; Turner, A.P.F. Lateral-Flow Technology: From Visual to Instrumental. *TrAC Trends Anal. Chem.* **2016**, *79*, 297–305. [[CrossRef](#)]
56. Younes, N.; Yassine, H.M.; Kourentzi, K.; Tang, P.; Litvinov, D.; Willson, R.C.; Abu-Raddad, L.J.; Nasrallah, G.K. A Review of Rapid Food Safety Testing: Using Lateral Flow Assay Platform to Detect Foodborne Pathogens. *Crit. Rev. Food Sci. Nutr.* **2023**, *12*, 1–23. [[CrossRef](#)] [[PubMed](#)]
57. Bahadır, E.B.; Sezginürk, M.K. Lateral Flow Assays: Principles, Designs and Labels. *TrAC Trends Anal. Chem.* **2016**, *82*, 286–306. [[CrossRef](#)]
58. Parolo, C.; Sena-Torralla, A.; Bergua, J.F.; Calucho, E.; Fuentes-Chust, C.; Hu, L.; Rivas, L.; Álvarez-Diduk, R.; Nguyen, E.P.; Cinti, S.; et al. Tutorial: Design and Fabrication of Nanoparticle-Based Lateral-Flow Immunoassays. *Nat. Protoc.* **2020**, *15*, 3788–3816. [[CrossRef](#)] [[PubMed](#)]
59. Santos, B.S.A.S.; Cunha, J.L.R.; Carvalho, I.C.; Costa, J.M.C.; Longo, B.C.; Galinari, G.C.F.; Diniz, P.H.S.M.; Mendes, G.M.M.; Fonseca, F.G.; Abrahão, J.S.; et al. Nanotechnology Meets Immunology towards a Rapid Diagnosis Solution: The COVID-19 Outbreak Challenge. *RSC Adv.* **2022**, *12*, 31711–31728. [[CrossRef](#)]
60. Pramanik, A.; Gao, Y.; Patibandla, S.; Gates, K.; Ray, P.C. Bioconjugated Nanomaterial for Targeted Diagnosis of SARS-CoV-2. *Acc. Mater. Res.* **2022**, *3*, 134–148. [[CrossRef](#)]
61. Derakhshan, M.A.; Amani, A.; Faridi-Majidi, R. State-of-the-Art of Nanodiagnostics and Nanotherapeutics against SARS-CoV-2. *ACS Appl. Mater. Interfaces* **2021**, *13*, 14816–14843. [[CrossRef](#)]
62. Shen, Y.; Shen, G. Signal-Enhanced Lateral Flow Immunoassay with Dual Gold Nanoparticle Conjugates for the Detection of Hepatitis B Surface Antigen. *ACS Omega* **2019**, *4*, 5083–5087. [[CrossRef](#)]
63. Toubanaki, D.K.; Margaroni, M.; Prapas, A.; Karagouni, E. Development of a Nanoparticle-Based Lateral Flow Strip Biosensor for Visual Detection of Whole Nervous Necrosis Virus Particles. *Sci. Rep.* **2020**, *10*, 6529. [[CrossRef](#)] [[PubMed](#)]
64. Huang, C.; Wen, T.; Shi, F.-J.; Zeng, X.-Y.; Jiao, Y.-J. Rapid Detection of IgM Antibodies against the SARS-CoV-2 Virus via Colloidal Gold Nanoparticle-Based Lateral-Flow Assay. *ACS Omega* **2020**, *5*, 12550–12556. [[CrossRef](#)] [[PubMed](#)]
65. Lee, A.S.; Kim, S.M.; Kim, K.R.; Park, C.; Lee, D.-G.; Heo, H.R.; Cha, H.J.; Kim, C.S. A Colorimetric Lateral Flow Immunoassay Based on Oriented Antibody Immobilization for Sensitive Detection of SARS-CoV-2. *Sens. Actuators B Chem.* **2023**, *379*, 133245. [[CrossRef](#)] [[PubMed](#)]

66. Cavalera, S.; Colitti, B.; Rosati, S.; Ferrara, G.; Bertolotti, L.; Nogarol, C.; Guiotto, C.; Cagnazzo, C.; Denina, M.; Fagioli, F.; et al. A Multi-Target Lateral Flow Immunoassay Enabling the Specific and Sensitive Detection of Total Antibodies to SARS-CoV-2. *Talanta* **2021**, *223*, 121737. [[CrossRef](#)] [[PubMed](#)]
67. Oh, H.-K.; Kim, K.; Park, J.; Im, H.; Maher, S.; Kim, M.-G. Plasmon Color-Preserved Gold Nanoparticle Clusters for High Sensitivity Detection of SARS-CoV-2 Based on Lateral Flow Immunoassay. *Biosens. Bioelectron.* **2022**, *205*, 114094. [[CrossRef](#)] [[PubMed](#)]
68. Rong, Z.; Wang, Q.; Sun, N.; Jia, X.; Wang, K.; Xiao, R.; Wang, S. Smartphone-Based Fluorescent Lateral Flow Immunoassay Platform for Highly Sensitive Point-of-Care Detection of Zika Virus Nonstructural Protein 1. *Anal. Chim. Acta* **2019**, *1055*, 140–147. [[CrossRef](#)] [[PubMed](#)]
69. Dong, T.; Zhang, X.; Yuan, J.; Lin, Z.; Yin, P.; Yu, H.; Wang, M.; Liu, A. Sensitive Lateral Flow Immunoassay Based on Specific Peptide and Superior Oxidase Mimics with a Universal Dual-Mode Significant Signal Amplification. *Anal. Chem.* **2023**, *95*, 12532–12540. [[CrossRef](#)] [[PubMed](#)]
70. Han, H.; Wang, C.; Yang, X.; Zheng, S.; Cheng, X.; Liu, Z.; Zhao, B.; Xiao, R. Rapid Field Determination of SARS-CoV-2 by a Colorimetric and Fluorescent Dual-Functional Lateral Flow Immunoassay Biosensor. *Sens. Actuators B Chem.* **2022**, *351*, 130897. [[CrossRef](#)]
71. Yu, Q.; Li, J.; Zheng, S.; Xia, X.; Xu, C.; Wang, C.; Wang, C.; Gu, B. Molybdenum Disulfide-Loaded Multilayer AuNPs with Colorimetric-SERS Dual-Signal Enhancement Activities for Flexible Immunochromatographic Diagnosis of Monkeypox Virus. *J. Hazard. Mater.* **2023**, *459*, 132136. [[CrossRef](#)]
72. Sena-Torralba, A.; Álvarez-Diduk, R.; Parolo, C.; Piper, A.; Merkoçi, A. Toward Next Generation Lateral Flow Assays: Integration of Nanomaterials. *Chem. Rev.* **2022**, *122*, 14881–14910. [[CrossRef](#)] [[PubMed](#)]
73. Zhang, J.; Gui, X.; Zheng, Q.; Chen, Y.; Ge, S.; Zhang, J.; Xia, N. An HRP-labeled Lateral Flow Immunoassay for Rapid Simultaneous Detection and Differentiation of Influenza A and B Viruses. *J. Med. Virol.* **2019**, *91*, 503–507. [[CrossRef](#)] [[PubMed](#)]
74. Axelrod, T.; Eltzov, E.; Marks, R.S. Capture-Layer Lateral Flow Immunoassay: A New Platform Validated in the Detection and Quantification of Dengue NS1. *ACS Omega* **2020**, *5*, 10433–10440. [[CrossRef](#)] [[PubMed](#)]
75. Ren, W.; Irudayaraj, J. Paper-Based Test for Rapid On-Site Screening of SARS-CoV-2 in Clinical Samples. *Biosensors* **2021**, *11*, 488. [[CrossRef](#)] [[PubMed](#)]
76. Huang, Y.; Ren, J.; Qu, X. Nanozymes: Classification, Catalytic Mechanisms, Activity Regulation, and Applications. *Chem. Rev.* **2019**, *119*, 4357–4412. [[CrossRef](#)] [[PubMed](#)]
77. Duan, D.; Fan, K.; Zhang, D.; Tan, S.; Liang, M.; Liu, Y.; Zhang, J.; Zhang, P.; Liu, W.; Qiu, X.; et al. Nanozyme-Strip for Rapid Local Diagnosis of Ebola. *Biosens. Bioelectron.* **2015**, *74*, 134–141. [[CrossRef](#)] [[PubMed](#)]
78. Liu, D.; Ju, C.; Han, C.; Shi, R.; Chen, X.; Duan, D.; Yan, J.; Yan, X. Nanozyme Chemiluminescence Paper Test for Rapid and Sensitive Detection of SARS-CoV-2 Antigen. *Biosens. Bioelectron.* **2021**, *173*, 112817. [[CrossRef](#)]
79. Panferov, V.G.; Safenkova, I.V.; Zherdev, A.V.; Dzantiev, B.B. The Steadfast Au@Pt Soldier: Peroxide-Tolerant Nanozyme for Signal Enhancement in Lateral Flow Immunoassay of Peroxidase-Containing Samples. *Talanta* **2021**, *225*, 121961. [[CrossRef](#)] [[PubMed](#)]
80. Sun, Y.; Xie, Z.; Pei, F.; Hu, W.; Feng, S.; Hao, Q.; Liu, B.; Mu, X.; Lei, W.; Tong, Z. Trimetallic Au@Pd@Pt Nanozyme-Enhanced Lateral Flow Immunoassay for the Detection of SARS-CoV-2 Nucleocapsid Protein. *Anal. Methods* **2022**, *14*, 5091–5099. [[CrossRef](#)]
81. Cheng, X.; Yang, X.; Tu, Z.; Rong, Z.; Wang, C.; Wang, S. Graphene Oxide-Based Colorimetric/Fluorescence Dual-Mode Immunochromatography Assay for Simultaneous Ultrasensitive Detection of Respiratory Virus and Bacteria in Complex Samples. *J. Hazard. Mater.* **2023**, *459*, 132192. [[CrossRef](#)]
82. Li, J.; Liang, P.; Zhao, T.; Guo, G.; Zhu, J.; Wen, C.; Zeng, J. Colorimetric and Raman Dual-Mode Lateral Flow Immunoassay Detection of SARS-CoV-2 N Protein Antibody Based on Ag Nanoparticles with Ultrathin Au Shell Assembled onto Fe₃O₄ Nanoparticles. *Anal. Bioanal. Chem.* **2023**, *415*, 545–554. [[CrossRef](#)]
83. Wang, C.; Yang, X.; Gu, B.; Liu, H.; Zhou, Z.; Shi, L.; Cheng, X.; Wang, S. Sensitive and Simultaneous Detection of SARS-CoV-2-Specific IgM/IgG Using Lateral Flow Immunoassay Based on Dual-Mode Quantum Dot Nanobeads. *Anal. Chem.* **2020**, *92*, 15542–15549. [[CrossRef](#)]
84. Liu, Y.; Lv, Y.; Chen, W.; Yang, X.; Cheng, X.; Rong, Z.; Wang, S. Development of a Fluorescent Immunochromatographic Assay Based on Quantum Dot-Functionalized Two-Dimensional Monolayer Ti₃C₂ MXene Nanoprobes for the Simultaneous Detection of Influenza A Virus and SARS-CoV-2. *ACS Appl. Mater. Interfaces* **2023**, *15*, 35872–35883. [[CrossRef](#)] [[PubMed](#)]
85. Liang, P.; Guo, Q.; Zhao, T.; Wen, C.-Y.; Tian, Z.; Shang, Y.; Xing, J.; Jiang, Y.; Zeng, J. Ag Nanoparticles with Ultrathin Au Shell-Based Lateral Flow Immunoassay for Colorimetric and SERS Dual-Mode Detection of SARS-CoV-2 IgG. *Anal. Chem.* **2022**, *94*, 8466–8473. [[CrossRef](#)]
86. Roberts, A.; Prakashan, D.; Dhanze, H.; Gandham, R.K.; Gandhi, S.; Sharma, G.T. Immuno-Chromatic Probe Based Lateral Flow Assay for Point-of-Care Detection of Japanese Encephalitis Virus NS1 Protein Biomarker in Clinical Samples Using a Smartphone-Based Approach. *Nanoscale Adv.* **2022**, *4*, 3966–3977. [[CrossRef](#)]
87. Panferov, V.G.; Safenkova, I.V.; Varitsev, Y.A.; Zherdev, A.V.; Dzantiev, B.B. Enhancement of Lateral Flow Immunoassay by Alkaline Phosphatase: A Simple and Highly Sensitive Test for Potato Virus X. *Microchim. Acta* **2018**, *185*, 25. [[CrossRef](#)] [[PubMed](#)]

88. Vafabakhsh, M.; Dadmehr, M.; Kazemi Noureini, S.; Es'haghi, Z.; Malekkiani, M.; Hosseini, M. Paper-Based Colorimetric Detection of COVID-19 Using Aptasenor Based on Biomimetic Peroxidase like Activity of ChF/ZnO/CNT Nano-Hybrid. *Spectrochim. Acta A Mol. Biomol. Spectrosc.* **2023**, *301*, 122980. [[CrossRef](#)]
89. Wang, K.; Liu, X.; Liang, X.; Jiang, Y.; Wen, C.-Y.; Zeng, J. Near-Infrared Responsive Ag@Au Nanoplates with Exceptional Stability for Highly Sensitive Colorimetric and Photothermal Dual-Mode Lateral Flow Immunoassay. *Anal. Chem.* **2024**, *96*, 3216. [[CrossRef](#)] [[PubMed](#)]
90. Atta, S.; Zhao, Y.; Li, J.Q.; Vo-Dinh, T. Dual-Modal Colorimetric and Surface-Enhanced Raman Scattering (SERS)-Based Lateral Flow Immunoassay for Ultrasensitive Detection of SARS-CoV-2 Using a Plasmonic Gold Nanocrown. *Anal. Chem.* **2024**, *96*, 4783–4790. [[CrossRef](#)]
91. Xu, L.-D.; Zhang, Q.; Ding, S.-N.; Xu, J.-J.; Chen, H.-Y. Ultrasensitive Detection of Severe Fever with Thrombocytopenia Syndrome Virus Based on Immunofluorescent Carbon Dots/SiO₂ Nanosphere-Based Lateral Flow Assay. *ACS Omega* **2019**, *4*, 21431–21438. [[CrossRef](#)]
92. Zhou, Y.; Chen, Y.; Liu, W.; Fang, H.; Li, X.; Hou, L.; Liu, Y.; Lai, W.; Huang, X.; Xiong, Y. Development of a Rapid and Sensitive Quantum Dot Nanobead-Based Double-Antigen Sandwich Lateral Flow Immunoassay and Its Clinical Performance for the Detection of SARS-CoV-2 Total Antibodies. *Sens. Actuators B Chem.* **2021**, *343*, 130139. [[CrossRef](#)] [[PubMed](#)]
93. Nguyen, A.V.T.; Dao, T.D.; Trinh, T.T.T.; Choi, D.-Y.; Yu, S.-T.; Park, H.; Yeo, S.-J. Sensitive Detection of Influenza a Virus Based on a CdSe/CdS/ZnS Quantum Dot-Linked Rapid Fluorescent Immunochromatographic Test. *Biosens. Bioelectron.* **2020**, *155*, 112090. [[CrossRef](#)] [[PubMed](#)]
94. Xu, L.-D.; Du, F.-L.; Zhu, J.; Ding, S.-N. Luminous Silica Colloids with Carbon Dot Incorporation for Sensitive Immunochromatographic Assay of Zika Virus. *Analyst* **2021**, *146*, 706–713. [[CrossRef](#)] [[PubMed](#)]
95. Bai, Z.; Wei, H.; Yang, X.; Zhu, Y.; Peng, Y.; Yang, J.; Wang, C.; Rong, Z.; Wang, S. Rapid Enrichment and Ultrasensitive Detection of Influenza A Virus in Human Specimen Using Magnetic Quantum Dot Nanobeads Based Test Strips. *Sens. Actuators B Chem.* **2020**, *325*, 128780. [[CrossRef](#)] [[PubMed](#)]
96. Kang, K.; Huang, L.; Ouyang, C.; Du, J.; Yang, B.; Chi, Y.; He, S.; Ying, L.; Chen, G.; Wang, J. Development, Performance Evaluation, and Clinical Application of a Rapid SARS-CoV-2 IgM and IgG Test Kit Based on Automated Fluorescence Immunoassay. *J. Med. Virol.* **2021**, *93*, 2838–2847. [[CrossRef](#)] [[PubMed](#)]
97. Chen, R.; Ren, C.; Liu, M.; Ge, X.; Qu, M.; Zhou, X.; Liang, M.; Liu, Y.; Li, F. Early Detection of SARS-CoV-2 Seroconversion in Humans with Aggregation-Induced Near-Infrared Emission Nanoparticle-Labeled Lateral Flow Immunoassay. *ACS Nano* **2021**, *15*, 8996–9004. [[CrossRef](#)] [[PubMed](#)]
98. Zhang, C.; Zhou, L.; Du, K.; Zhang, Y.; Wang, J.; Chen, L.; Lyu, Y.; Li, J.; Liu, H.; Huo, J.; et al. Foundation and Clinical Evaluation of a New Method for Detecting SARS-CoV-2 Antigen by Fluorescent Microsphere Immunochromatography. *Front. Cell. Infect. Microbiol.* **2020**, *10*, 553837. [[CrossRef](#)] [[PubMed](#)]
99. Mao, M.; Wu, F.; Shi, X.; Huang, Y.; Ma, L. Ultrasensitive Detection of COVID-19 Virus N Protein Based on p-Toluenesulfonyl Modified Fluorescent Microspheres Immunoassay. *Biosensors* **2022**, *12*, 437. [[CrossRef](#)]
100. Wei-Wen Hsiao, W.; Sharma, N.; Le, T.-N.; Cheng, Y.-Y.; Lee, C.-C.; Vo, D.-T.; Hui, Y.Y.; Chang, H.-C.; Chiang, W.-H. Fluorescent Nanodiamond-Based Spin-Enhanced Lateral Flow Immunoassay for Detection of SARS-CoV-2 Nucleocapsid Protein and Spike Protein from Different Variants. *Anal. Chim. Acta* **2022**, *1230*, 340389. [[CrossRef](#)]
101. Xu, G.; Zeng, S.; Zhang, B.; Swihart, M.T.; Yong, K.-T.; Prasad, P.N. New Generation Cadmium-Free Quantum Dots for Biophotonics and Nanomedicine. *Chem. Rev.* **2016**, *116*, 12234–12327. [[CrossRef](#)]
102. Chen, Z.; Zhang, Z.; Zhai, X.; Li, Y.; Lin, L.; Zhao, H.; Bian, L.; Li, P.; Yu, L.; Wu, Y.; et al. Rapid and Sensitive Detection of Anti-SARS-CoV-2 IgG, Using Lanthanide-Doped Nanoparticles-Based Lateral Flow Immunoassay. *Anal. Chem.* **2020**, *92*, 7226–7231. [[CrossRef](#)] [[PubMed](#)]
103. Le, T.-N.; Hsiao, W.W.-W.; Cheng, Y.-Y.; Lee, C.-C.; Huynh, T.-T.; Pham, D.M.; Chen, M.; Jen, M.-W.; Chang, H.-C.; Chiang, W.-H. Spin-Enhanced Lateral Flow Immunoassay for High-Sensitivity Detection of Nonstructural Protein NS1 Serotypes of the Dengue Virus. *Anal. Chem.* **2022**, *94*, 17819–17826. [[CrossRef](#)]
104. Hong, D.; Jo, E.-J.; Bang, D.; Jung, C.; Lee, Y.E.; Noh, Y.-S.; Shin, M.G.; Kim, M.-G. Plasmonic Approach to Fluorescence Enhancement of Mesoporous Silica-Coated Gold Nanorods for Highly Sensitive Influenza A Virus Detection Using Lateral Flow Immunosensor. *ACS Nano* **2023**, *17*, 16607–16619. [[CrossRef](#)] [[PubMed](#)]
105. Fu, H.E.; Koo, T.M.; Kim, M.S.; Ko, M.J.; Park, B.C.; Oh, K.; Cho, Y.; Jung, J.-W.; Kim, S.; Jang, W.S.; et al. Magnetic-Fluorescent Nanocluster Lateral Flow Assay for Rotavirus Detection. *ACS Appl. Nano Mater.* **2023**, *6*, 5789–5798. [[CrossRef](#)]
106. Zhou, J.; Yang, Y.; Zhang, C. Toward Biocompatible Semiconductor Quantum Dots: From Biosynthesis and Bioconjugation to Biomedical Application. *Chem. Rev.* **2015**, *115*, 11669–11717. [[CrossRef](#)] [[PubMed](#)]
107. Wang, C.; Cheng, X.; Liu, L.; Zhang, X.; Yang, X.; Zheng, S.; Rong, Z.; Wang, S. Ultrasensitive and Simultaneous Detection of Two Specific SARS-CoV-2 Antigens in Human Specimens Using Direct/Enrichment Dual-Mode Fluorescence Lateral Flow Immunoassay. *ACS Appl. Mater. Interfaces* **2021**, *13*, 40342–40353. [[CrossRef](#)] [[PubMed](#)]
108. Li, Z.; Wang, A.; Zhou, J.; Chen, Y.; Liu, H.; Liu, Y.; Zhang, Y.; Ding, P.; Zhu, X.; Liang, C.; et al. A Universal Fluorescent Immunochromatography Assay Based on Quantum Dot Nanoparticles for the Rapid Detection of Specific Antibodies against SARS-CoV-2 Nucleocapsid Protein. *Int. J. Mol. Sci.* **2022**, *23*, 6225. [[CrossRef](#)] [[PubMed](#)]

109. Chen, W.; Chen, H.; Liu, Y.; Wei, H.; Wang, Y.; Rong, Z.; Liu, X. An Integrated Fluorescent Lateral Flow Assay for Multiplex Point-of-Care Detection of Four Respiratory Viruses. *Anal. Biochem.* **2022**, *659*, 114948. [[CrossRef](#)] [[PubMed](#)]
110. Srivastav, S.; Dankov, A.; Adanalic, M.; Grzeschik, R.; Tran, V.; Pagel-Wieder, S.; Gessler, F.; Spreitzer, I.; Scholz, T.; Schmierle, B.; et al. Rapid and Sensitive SERS-Based Lateral Flow Test for SARS-CoV-2-Specific IgM/IgG Antibodies. *Anal. Chem.* **2021**, *93*, 12391–12399. [[CrossRef](#)] [[PubMed](#)]
111. Lu, M.; Joung, Y.; Jeon, C.S.; Kim, S.; Yong, D.; Jang, H.; Pyun, S.H.; Kang, T.; Choo, J. Dual-Mode SERS-Based Lateral Flow Assay Strips for Simultaneous Diagnosis of SARS-CoV-2 and Influenza A Virus. *Nano Converg.* **2022**, *9*, 39. [[CrossRef](#)]
112. Borzenkov, M.; Chirico, G.; D'Alfonso, L.; Sironi, L.; Collini, M.; Cabrini, E.; Dacarro, G.; Milanese, C.; Pallavicini, P.; Taglietti, A.; et al. Thermal and Chemical Stability of Thiol Bonding on Gold Nanostars. *Langmuir* **2015**, *31*, 8081–8091. [[CrossRef](#)] [[PubMed](#)]
113. Lu, X.; Mei, T.; Guo, Q.; Zhou, W.; Li, X.; Chen, J.; Zhou, X.; Sun, N.; Fang, Z. Improved Performance of Lateral Flow Immunoassays for Alpha-Fetoprotein and Vanillin by Using Silica Shell-Stabilized Gold Nanoparticles. *Microchim. Acta* **2019**, *186*, 2. [[CrossRef](#)] [[PubMed](#)]
114. Wang, F.; Widejko, R.G.; Yang, Z.; Nguyen, K.T.; Chen, H.; Fernando, L.P.; Christensen, K.A.; Anker, J.N. Surface-Enhanced Raman Scattering Detection of PH with Silica-Encapsulated 4-Mercaptobenzoic Acid-Functionalized Silver Nanoparticles. *Anal. Chem.* **2012**, *84*, 8013–8019. [[CrossRef](#)] [[PubMed](#)]
115. Jeon, J.; Lee, S.H.; Joung, Y.; Kim, K.; Choi, N.; Choo, J. Improvement of Reproducibility and Thermal Stability of Surface-Enhanced Raman Scattering-Based Lateral Flow Assay Strips Using Silica-Encapsulated Gold Nanoparticles. *Sens. Actuators B Chem.* **2020**, *321*, 128521. [[CrossRef](#)]
116. Liu, H.; Dai, E.; Xiao, R.; Zhou, Z.; Zhang, M.; Bai, Z.; Shao, Y.; Qi, K.; Tu, J.; Wang, C.; et al. Development of a SERS-Based Lateral Flow Immunoassay for Rapid and Ultra-Sensitive Detection of Anti-SARS-CoV-2 IgM/IgG in Clinical Samples. *Sens. Actuators B Chem.* **2021**, *329*, 129196. [[CrossRef](#)] [[PubMed](#)]
117. Zhang, Y.; Wu, G.; Wei, J.; Ding, Y.; Wei, Y.; Liu, Q.; Chen, H. Rapid and Sensitive Detection of Rotavirus by Surface-Enhanced Raman Scattering Immunochromatography. *Microchim. Acta* **2021**, *188*, 3. [[CrossRef](#)] [[PubMed](#)]
118. Jia, X.; Liu, Z.; Peng, Y.; Hou, G.; Chen, W.; Xiao, R. Automatic and Sensitive Detection of West Nile Virus Non-Structural Protein 1 with a Portable SERS-LFIA Detector. *Microchim. Acta* **2021**, *188*, 206. [[CrossRef](#)] [[PubMed](#)]
119. Liang, J.; Wu, L.; Wang, Y.; Liang, W.; Hao, Y.; Tan, M.; He, G.; Lv, D.; Wang, Z.; Zeng, T.; et al. SERS/Photothermal-Based Dual-Modal Lateral Flow Immunoassays for Sensitive and Simultaneous Antigen Detection of Respiratory Viral Infections. *Sens. Actuators B Chem.* **2023**, *389*, 133875. [[CrossRef](#)]
120. Shen, H.; Xie, K.; Huang, L.; Wang, L.; Ye, J.; Xiao, M.; Ma, L.; Jia, A.; Tang, Y. A Novel SERS-Based Lateral Flow Assay for Differential Diagnosis of Wild-Type Pseudorabies Virus and GE-Deleted Vaccine. *Sens. Actuators B Chem.* **2019**, *282*, 152–157. [[CrossRef](#)]
121. Xiao, M.; Xie, K.; Dong, X.; Wang, L.; Huang, C.; Xu, F.; Xiao, W.; Jin, M.; Huang, B.; Tang, Y. Ultrasensitive Detection of Avian Influenza A (H7N9) Virus Using Surface-Enhanced Raman Scattering-Based Lateral Flow Immunoassay Strips. *Anal. Chim. Acta* **2019**, *1053*, 139–147. [[CrossRef](#)]
122. Shen, H.; Song, E.; Wang, Y.; Meng, L.; Dong, J.; Lin, B.; Huang, D.; Guan, Z.; Yang, C.; Zhu, Z. In Situ Raman Enhancement Strategy for Highly Sensitive and Quantitative Lateral Flow Assay. *Anal. Bioanal. Chem.* **2022**, *414*, 507–513. [[CrossRef](#)] [[PubMed](#)]
123. Gandra, N.; Hendargo, H.C.; Norton, S.J.; Fales, A.M.; Palmer, G.M.; Vo-Dinh, T. Tunable and Amplified Raman Gold Nanoprobes for Effective Tracking (TARGET): In Vivo Sensing and Imaging. *Nanoscale* **2016**, *8*, 8486–8494. [[CrossRef](#)]
124. Ngo, H.T.; Gandra, N.; Fales, A.M.; Taylor, S.M.; Vo-Dinh, T. Sensitive DNA Detection and SNP Discrimination Using Ultrabright SERS Nanorattles and Magnetic Beads for Malaria Diagnostics. *Biosens. Bioelectron.* **2016**, *81*, 8–14. [[CrossRef](#)] [[PubMed](#)]
125. Yap, L.W.; Chen, H.; Gao, Y.; Petkovic, K.; Liang, Y.; Si, K.J.; Wang, H.; Tang, Z.; Zhu, Y.; Cheng, W. Bifunctional Plasmonic-Magnetic Particles for an Enhanced Microfluidic SERS Immunoassay. *Nanoscale* **2017**, *9*, 7822–7829. [[CrossRef](#)] [[PubMed](#)]
126. Wang, C.; Wang, J.; Li, P.; Rong, Z.; Jia, X.; Ma, Q.; Xiao, R.; Wang, S. Sonochemical Synthesis of Highly Branched Flower-like Fe₃O₄@SiO₂@Ag Microcomposites and Their Application as Versatile SERS Substrates. *Nanoscale* **2016**, *8*, 19816–19828. [[CrossRef](#)] [[PubMed](#)]
127. Wang, Y.; Gao, T.; Wang, K.; Zou, B.; Zhang, X.; Du, Z.; Zhou, S. Magnetic-Based Silver Composite Microspheres with Nanosheet-Assembled Shell for Effective SERS Substrate. *J. Mater. Chem. C Mater.* **2013**, *1*, 2441–2447. [[CrossRef](#)]
128. Wang, C.; Wang, C.; Wang, X.; Wang, K.; Zhu, Y.; Rong, Z.; Wang, W.; Xiao, R.; Wang, S. Magnetic SERS Strip for Sensitive and Simultaneous Detection of Respiratory Viruses. *ACS Appl. Mater. Interfaces* **2019**, *11*, 19495–19505. [[CrossRef](#)] [[PubMed](#)]
129. Xie, Z.; Feng, S.; Pei, F.; Xia, M.; Hao, Q.; Liu, B.; Tong, Z.; Wang, J.; Lei, W.; Mu, X. Magnetic/Fluorescent Dual-Modal Lateral Flow Immunoassay Based on Multifunctional Nanobeads for Rapid and Accurate SARS-CoV-2 Nucleocapsid Protein Detection. *Anal. Chim. Acta* **2022**, *1233*, 340486. [[CrossRef](#)] [[PubMed](#)]
130. Liu, Z.; Wang, C.; Zheng, S.; Yang, X.; Han, H.; Dai, Y.; Xiao, R. Simultaneously Ultrasensitive and Quantitative Detection of Influenza A Virus, SARS-CoV-2, and Respiratory Syncytial Virus via Multichannel Magnetic SERS-Based Lateral Flow Immunoassay. *Nanomedicine* **2023**, *47*, 102624. [[CrossRef](#)]
131. Liu, X.; Yang, X.; Wang, C.; Liu, Q.; Ding, Y.; Xu, S.; Wang, G.; Xiao, R. A Nanogap-Enhanced SERS Nanotag-Based Lateral Flow Assay for Ultrasensitive and Simultaneous Monitoring of SARS-CoV-2 S and NP Antigens. *Microchim. Acta* **2024**, *191*, 104. [[CrossRef](#)]

132. Huang, L.; Tian, S.; Zhao, W.; Liu, K.; Ma, X.; Guo, J. Multiplexed Detection of Biomarkers in Lateral-Flow Immunoassays. *Analyst* **2020**, *145*, 2828–2840. [[CrossRef](#)] [[PubMed](#)]
133. Ghasemi, F.; Fahimi-Kashani, N.; Bigdeli, A.; Alshatteri, A.H.; Abbasi-Moayed, S.; Al-Jaf, S.H.; Merry, M.Y.; Omer, K.M.; Hormozi-Nezhad, M.R. Paper-Based Optical Nanosensors—A Review. *Anal. Chim. Acta* **2023**, *1238*, 340640. [[CrossRef](#)] [[PubMed](#)]
134. Liu, J.; Li, M.; Man, Q.; Huang, L.; Wang, J.; Gao, M.; Zhang, X. Naked-Eye Readout Distance Quantitative Lateral Flow Assay Based on the Permeability Changes of Enzyme-Catalyzed Hydrogelation. *Anal. Chem.* **2023**, *95*, 8011–8019. [[CrossRef](#)] [[PubMed](#)]
135. Kim, S.K.; Lee, J.U.; Jeon, M.J.; Kim, S.-K.; Hwang, S.-H.; Hong, M.E.; Sim, S.J. Bio-Conjugated Nanoarchitectonics with Dual-Labeled Nanoparticles for a Colorimetric and Fluorescent Dual-Mode Serological Lateral Flow Immunoassay Sensor. *RSC Adv.* **2023**, *13*, 27225–27232. [[CrossRef](#)] [[PubMed](#)]
136. Misawa, K.; Yamamoto, T.; Hiruta, Y.; Yamazaki, H.; Citterio, D. Text-Displaying Semiquantitative Competitive Lateral Flow Immunoassay Relying on Inkjet-Printed Patterns. *ACS Sens.* **2020**, *5*, 2076–2085. [[CrossRef](#)]
137. Yang, D.; Hu, C.; Zhang, H.; Geng, S. Recent Developments in Paper-Based Sensors with Instrument-Free Signal Readout Technologies (2020–2023). *Biosensors* **2024**, *14*, 36. [[CrossRef](#)]

Disclaimer/Publisher’s Note: The statements, opinions and data contained in all publications are solely those of the individual author(s) and contributor(s) and not of MDPI and/or the editor(s). MDPI and/or the editor(s) disclaim responsibility for any injury to people or property resulting from any ideas, methods, instructions or products referred to in the content.